THE MOLECULAR ROLE OF MOB1 IN LATS1 KINASE ACTIVATION IN HIPPO SIGNALING

by

Yoo Jin Kim

A thesis submitted to Johns Hopkins University in conformity with the requirements for the degree of Master of Science

Baltimore, Maryland

May 2018

Abstract

The Hippo signaling pathway, a highly conserved pathway between flies and mammals, regulates the rate of cell growth and apoptosis to ultimately control organ size and tissue homeostasis (Saucedo & Edgar, 2007). The pathway was named after an overgrowth phenotype, a fly resembling a hippopotamus, observed in Drosophila upon mutating *Hpo* (Wu et al., 2003). The action of the Hippo pathway arises from the activity of a set of two kinases. Mst1/2 kinase phosphorylates and activates Lats1/2 kinase in a process that may be stimulated by the effector protein Mob1, which is also a substrate of Mst1/2 (Ni et al., 2015). This study aims to identify a minimal, functional unit of Lats1 more amenable to both purification *in vitro* and X-ray crystallization. We designed truncations of both the N and C-termini of Lats1. We transiently transfected Mst2, Mob1, Lats1, and YAP in HEK293 cells and validated kinase activity of the truncated Lats1 variants by Western blot and the luciferase reporter assay. We also analyzed complex formation between Mob1 and the truncated Lats1 variants using co-immunoprecipitation from lysate of HEK293 cells transiently transfected with both proteins. We will purify the minimal, functional unit of Lats1 *in vitro* for use in future biochemical and structural assays. This study also aims to understand the molecular role of Mob1 in the activation of Lats1 kinase. We transiently transfected HEK293 cells with Mst2 and Lats1 with or without Mob1 and monitored Lats1 activation by Western blot. Expression of Mob1 stimulated phosphorylation of Lats1 by Mst2, highlighting a potential role for Mob1 in Lats1 activation and ternary complex formation between Lats1, Mob1, and Mst2. We aim to isolate the ternary complex *in vitro* and test the phosphospecific nature of assembly of the ternary complex. We will also determine the sequence of molecular events that lead to

Lats1 activation by systematically disrupting pairwise interactions between either Mst2 and Mob1 or Lats1 and Mob1 and monitor the effect on Lats1 activation in cells. Several studies have identified mutations in human cancers that affect Lats1/2 expression and kinase activity (Yu, Bachman & Lai, 2013). Thus, the results of this study will provide insight into the mechanisms that regulate Lats1 activation and provide a framework to guide targeted molecular therapies.

Advisor: Jennifer M. Kavran, Ph.D.

Thesis Reader: Anthony K. L. Leung, Ph.D.

Acknowledgements

First, I would like to thank Dr. Jennifer M. Kavran, my advisor and mentor during these past two years. I feel incredibly lucky to have met her. I have asked more questions, thought more critically, and felt more motivated because of her invaluable mentorship and unending patience. I aspire to share her enthusiasm and passion for scientific research throughout my career.

I would like to thank Dr. Floyd Bryant. His mentorship during my first year of this program gave me the confidence to pursue a Master of Science, and he has continuously supported me with every step of this experience. I would also like to thank Dr. Anthony Leung for his advice with this manuscript.

I would like to recognize the members of the Kavran Lab. I want to thank Dr. Thao Tran. Thao helped me to pursue my interests and was always eager to answer my questions, even those asked at odd hours of the night. I want to recognize Leah Cairns and Thomas Koehler for their help with this manuscript. Also, their friendship and support have been invaluable throughout my time at the Kavran Lab. I would also like to recognize Brendan Fowl for his help with the identification of the minimal, functional unit of Lats1 kinase and his completion of the luciferase assay.

Finally, I would like to thank my friends and family. I would like to acknowledge Alisa Boyko. She has inspired me to emulate her incredible passion for scientific research and the warmth and care she shares with others. I want to thank Stephen Reginald Wellard for the encouragement he shared and his tireless effort editing this manuscript. Most importantly, I would like to recognize my mother, Hee Jung Kim, and father, Yong Ha Kim. They are my role models, and their dedication and passion to both their work

and our family motivate me every day. I would not be here today without their love and constant support.

Table of Contents

List of Tables

List of Figures

Introduction

Genetic screens in *Drosophila melanogaster* led to the discovery of the Hippo tumor suppressor pathway. In Drosophila, mutations in *Hippo* (*hpo*), *Warts* (*wts*), or *mats* led to unregulated cell proliferation and an overgrowth phenotype (**Figure 1.1**) (Justice et al., 1995; Udan et al., 2003; Lai et al., 2005). The Hippo pathway is conserved in flies and mammals. Not only so, but expression of mammalian homologs of key Hippo pathway components can also rescue the overgrowth phenotype in knock-out Drosophila mutants. In mammals, the components of the Hippo pathway are named differently (**Table 1.1**). Here, we will refer to the mammalian nomenclature of the Hippo pathway.

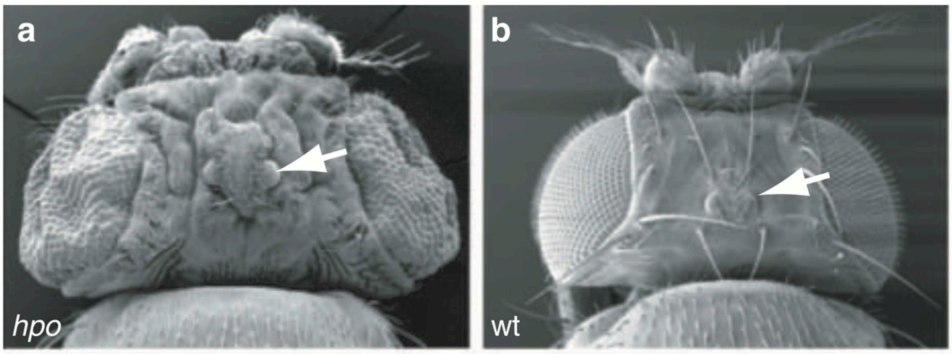

Figure 1.1: Mutating *hpo* causes overgrowth phenotype observed in *Drosophila melanogaster*
Mutagenic screens of *Drosophila melanogaster* isolated *Hpo* as a gene responsible for inducing an overgrowth tissue phenotype. Figure is adapted from (Udan et al., 2003).

Table 1.1: Nomenclature of mammalian and Drosophila homologues of the Hippo pathway

Drosophila Homolog	Mammalian Homolog
Hippo	Mst1/2
Warts	Lats1/2
Mats	Mob

Yes-associated Protein (YAP) was identified as the downstream target of Hippo signaling (Hao et al., 2008). YAP is a transcription-factor that associates with TEA-domain (TEAD) transcription factor in the nucleus to stimulate the expression of genes related to cell proliferation (Hao et al., 2008; Zhao et al., 2008). Hippo signaling regulates the localization of YAP to depress proliferative signals and promote apoptosis (Hao et al., 2008).

Since the discovery of the key Hippo pathway components, many studies have provided insight into the interactions that mediate Hippo signaling. The Hippo pathway core kinase cassette is shown in **Figure 1.2**. Mammalian sterile20 like kinase (Mst1/2) is a serine/threonine kinase. Mst1/2 phosphorylates both Mob, a co-activator, and Large tumor suppressor (Lats1/2) kinase (Chan et al., 2005; Praskova et al., 2008). Mst1/2 phosphorylates Lats1/2 kinase, and this modification is necessary for Lats1/2 kinase activation (Chan et al., 2005). Mob1 binds Lats1/2 and stimulates Lats1/2 kinase activity (Hergovich, Schmitz & Hemmings, 2006). Activated Lats1/2 kinase phosphorylates YAP at residue S127 resulting in sequestration of YAP from the nucleus (Hao et al., 2008). Flies expressing mutant YAP S127A display an overgrowth phenotype (Dong et al., 2007). This result further validates the importance of Hippo signaling in regulating tissue homeostasis through inhibitory phosphorylation of YAP.

Aberrant Hippo signaling, such as increased YAP expression and deactivation or loss of *Lats1/2*, have been identified in many different human cancers (Halder & Johnson, 2010). Not only has Hippo signaling been associated with tumorigenesis but recent studies have also identified a possible role of Hippo signaling in tissue regeneration (Halder & Johnson, 2010). Following partial hepatectomy in rats, YAP

protein level increases in the liver (Wang et al., 2011). Also, the overgrowth phenotype caused by YAP overexpression in mice liver can be reversed by silencing YAP overexpression (Camargo et al., 2007; Dong et al., 2007). In humans, Hippo signaling changes in response to liver damage as detected by YAP localization to the nucleus (Bai et al., 2012). Thus, the applications of the Hippo pathway are vast, ranging from the development of therapeutic targets to combat tumorigenesis and use in tissue regeneration following injury.

Here, we are interested in the molecular mechanism for Lats1/2 kinase activation. Lats1/2 kinase phosphorylates YAP to sequester YAP, the downstream target of Hippo signaling, from the nucleus. First, we aim to define a minimal, functional unit of Lats1 kinase for use in future biochemical and structural assays. Much of the N and C-termini of Lats1/2 is disordered that is problematic for X-ray crystallization. Next, we aim to elucidate the molecular role of Mob1 in the activation of Lats1 kinase. Mob1 associates with both Mst2 and Lats1, the two key kinases of the Hippo pathway core kinase cassette. By elucidating the role that Mob1 plays in Hippo signaling, we will better understand the regulation of Lats1 kinase.

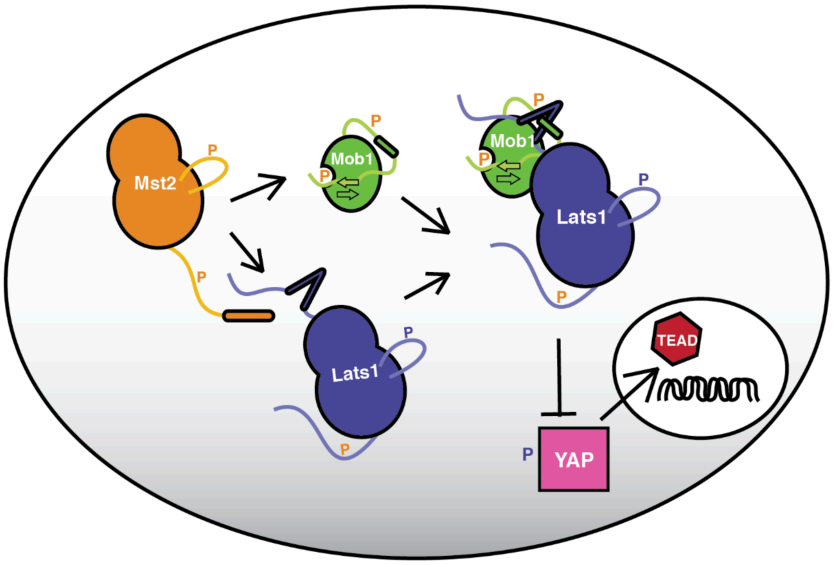

Figure 1.2: Schematic of Hippo pathway core kinase cassette
Mst1/2 kinase phosphorylates both Mob and Lats1/2 kinase (Chan et al., 2005; Praskova et al., 2008). Phosphorylation of Lats1/2 kinase by Mst1/2 is necessary for Lats1/2 kinase activation (Chan et al., 2005). Mob1 binds Lats1/2 kinase that stimulates Lats1/2 kinase activity (Hergovich, Schmitz & Hemmings, 2006). Active Lats1/2 kinase phosphorylates YAP thus sequestering YAP from the nucleus (Zhao et al., 2008). When unphosphorylated, YAP translocates to the nucleus and associates with TEAD to induce downstream proliferative signals (Hao et al., 2008).

Defining the minimal, functional unit of Lats1 kinase

Introduction

The Hippo pathway controls cell proliferation through cytoplasmic sequestration of the transcriptional coactivator YAP (Hao et al., 2008). Lats1/2, a key kinase in the core kinase cassette of the Hippo pathway, is responsible for the phosphorylation of YAP that prevents nuclear translocation (Hao et al., 2008). Despite the roles that Lats1/2 has been shown to play in tumorigenesis and cell cycle regulation, our understanding of the structure and function of Lats1/2 kinase is limited.

Lats1/2 kinase is part of the LATS/NDR (Nuclear dbf2-Related) kinase family, a subclass of the AGC serine/threonine kinase superfamily (Tamaskovic et al., 2003). AGC kinases are named after cAMP-dependent protein kinase 1 (PKA), cGMP-dependent protein kinase (PKG), and protein kinase C (PKC). AGC kinases share sequence similarity within the kinase domain (Pearce et al., 2010). The kinase domain takes the shape of a bilobal kinase fold: a smaller lobe that is N-terminal and a larger C-terminal lobe. Two other regions are also conserved amongst most AGC kinases: the activation loop within the kinase domain and the hydrophobic motif, which lies C-terminal to the kinase domain (**Figure 2.1**). Most AGC kinases also share a mechanism for kinase activation. Phosphorylation of two conserved regions, the activation loop and hydrophobic motif, regulate kinase activity (**Figure 2.1**) (Pearce et al., 2010).

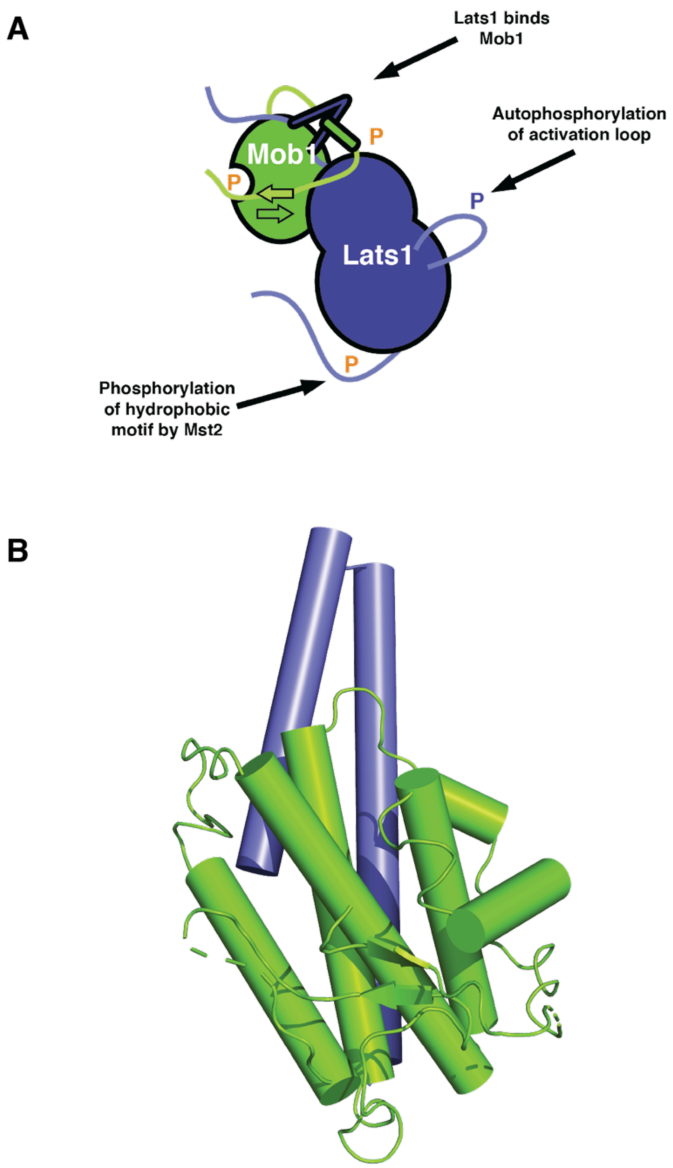

Figure 2.1: Structure and activation of Lats1 kinase
A. Three key events occur for Lats1 kinase activation. Mst2 phosphorylates the hydrophobic motif C-terminal to the Lats1 kinase domain (Chan et al., 2005). Lats1 autophosphorylates a conserved residue in the activation loop within the kinase domain (Chan et al., 2005). Lats1 binds Mob1, a co-activator, that stimulates both Lats1 autophosphorylation and substrate phosphorylation (Hergovich, Schmitz & Hemmings, 2013). **B.** Structure of Lats1 MBD (602-704) bound to phosphorylated Mob1 (pMob1) (Ni et al., 2015). Lats1 is represented in blue, and pMob1 is represented in green.

Like most AGC kinases, Lats1/2 kinase is regulated by phosphorylation at the hydrophobic motif and activation loop. Chan et al. identified Mst1/2 kinase as the kinase responsible for phosphorylating Lats1/2 at the hydrophobic motif (Chan et al., 2005).

Mst1/2 phosphorylation of the hydrophobic motif triggers Lats1/2 autophosphorylation of the activation loop (Chan et al., 2005). Multiple studies have demonstrated that phosphorylation of the hydrophobic motif and activation loop are necessary for Lats1/2 kinase activity (Chan et al., 2005; Hergovich, Schmitz & Hemmings, 2006; Hoa et al., 2016).

A hallmark of NDR kinases is an interaction with an allosteric activator from the Mob family of proteins. N-terminal to the kinase domain, each NDR kinase has a conserved Mob binding domain (MBD). However not all Mob proteins bind all NDR family kinases (Bichsel et al., 2004; Devroe et al., 2004; Kohler et al., 2010). Only Mob1 binds Lats1/2, and binding between Lats1/2 and Mob1 stimulates Lats1/2 autophosphorylation and substrate phosphorylation. The interaction between Mob1 and Lats1/2 is also observed in the Drosophila homologs – binding between Mats and Warts stimulates Warts kinase activity (Wei, Shimizu & Lai, 2007; Vrabioiu & Struhl, 2015). Mutational analysis further confirms the importance of Mob1 binding to Lats1/2. If the Mob1 and Lats1/2 binding interaction is inhibited, autophosphorylation and substrate phosphorylation by Lats1/2 significantly decreases compared to wild-type (wt) Lats1/2 (Hergovich, Schmitz & Hemmings, 2006; Ni et al., 2015; Hoa et al., 2016). In summary, three components are critical for Lats1/2 kinase activation: phosphorylation of the hydrophobic motif by Mst1/2, autophosphorylation of the activation loop, and binding to Mob1, a co-activator (**Figure 2.1**).

A long-term goal of this project is to determine the minimal, functional unit of Lats1 for use in biochemical and structural studies. Lats1 has a 712 amino acid long N-terminal region. The majority of the N-terminal region is predicted to be disordered by

secondary structure predictions and is not conserved between Lats1/2 homologs (**Figure 2.2**). Currently, the available structural data of Lats1 is limited to the MBD. Ni et al. resolved residues 602 – 703, and Kim et al. resolved residues 621 – 703 within the MBD (Ni et al., 2015; Kim et al., 2016). Thus, the reason to determine a minimal variant of Lats1 is that full-length Lats1 (127kDa) has proven technically challenging to express and purify *in vitro*. We also identified four functions that a minimal Lats1 needs to maintain based on available cellular and genetic data: hydrophobic motif phosphorylation, autophosphorylation of its activation loop, binding to a co-activator, Mob1, and phosphorylation of downstream components to maintain Hippo pathway function.

Materials and Methods

Cloning of Lats1 variants

The N-terminal truncated, C-terminal truncated, and kinase-dead (kd) (D827N) Lats1 variants were cloned using standard mutagenesis in pcDNA-3.1/3XMyc-Lats1 (Addgene) (**Table 2.6**). All variants were confirmed by DNA sequencing.

Sequence and structural analysis

Clustal Omega was used to perform sequence alignments between Lats1, Lats2, and Warts (Slevers et al., 2011). Secondary structure of Lats1 was predicted using JPred4 (Alexey Drozdetskiy et al., 2015).

Transient transfection of HEK293 cells

HEK293T cells were cultured in DMEM medium (Gibco) supplemented with 5% FBEssence (VWR) and 2mM Glutamine (Thermo Fischer) and grown at 37℃ and 5% CO_2. HEK293T cells were seeded and transiently transfected one day later using polyethylenimine hydrochloride transfection reagent (PEI Max, Polysciences Inc.) at a ratio of 3µl of PEI Max to 1µg of DNA. Seeding densities are reported in **Table 2.1**. The pcDNA plasmids transfected are indicated in **Table 2.2** and **Table 2.3**. 48 hours after transfection, cell medium was aspirated, and cells were washed with 1mL ice-cold phosphate-buffered saline (PBS). PBS was aspirated, and cells were incubated with ice-cold immunoprecipitation buffer (IP buffer) (20mM Tris pH 8.0, 150mM NaCl, 1% Nonidet P-40 (NP-40), and 10% glycerol) supplemented with 50mM NaF, 1mM Na_3VO_4, 0.5mM PMSF, and Pierce Universal Nuclease (Thermo Scientific, 1:10,000) while

rocking for 30 minutes at 4℃. Cell lysates were clarified by centrifugation at 23,000rpm for 10 minutes at 4℃. The total protein concentration in the lysate of each sample was quantified using the Pierce BCA protein assay kit (Thermo Scientific).

Table 2.1: Seeding density of HEK293 cells and total DNA transiently transfected

Experiment	Dish/Plate	Seeding Density	Total DNA Transfected (ug)
Co-Immunoprecipitation	60mm Dish	0.9*10^6	3
Substrate Phosphorylation	6-Well Plate	0.6*10^6	2

Table 2.2: Plasmids transfected in HEK293 cells for co-immunoprecipitation assay

Protein	Epitope Tag	Vector	Kavran Lab Code	DNA Transfected (ng)/Dish
Lats1	Myc	pcDNA	97	2400
Mob1	HA	pcDNA	96	600

Table 2.3 Plasmids transfected in HEK293 cells for Lats1 substrate phosphorylation assay

Protein	Epitope Tag	Vector	Kavran Lab Code	DNA Transfected (ng)/Well
Lats1	Myc	pcDNA	97	1000
Mob1	HA	pcDNA	96	333
Mst2	HA	pcDNA	94	333
YAP2	FLAG	pcDNA	122	333

Co-immunoprecipitation

The materials and methods detailed in the co-immunoprecipitation chapter were used. α-HA (Roche) antibody was used.

Western blot analysis

Samples were resolved on 10 or 15% sodium dodecyl sulfate-polyacrylamide gel electrophoresis (SDS-PAGE) and transferred to nitrocellulose membranes (0.45µm) using the Trans-Blot Turbo Transfer System (Bio-Rad). Membranes were blocked in 5%

skimmed milk powder in Tris-buffered saline (TBS: 20mM Tris pH 7.6 and 150mM NaCl) for 30 minutes at room temperature. Membranes were probed with primary antibodies overnight at 4℃ (**Table 2.4**). Membranes were washed three times with TBS-T (20mM Tris pH 7.6, 150mM NaCl, and 0.1% Tween-20) for 5 minutes. Then, membranes were incubated with fluorophore-conjugated secondary antibodies for 1 hour at room temperature (**Table 2.4**). The membranes were washed three times with TBS-T for 5 minutes. Blots were scanned on an Odyssey Infrared Imaging System (LI-COR) and analyzed using ImageStudio software (LI-COR).

Table 2.4: Antibodies used for Western blot analysis

Antibody	Host	Source	Reference	Dilution	Dilution Buffer	Repeated Use of Antibody?
c-Myc (9E10)	Mouse	Santa Cruz	sc-40	1:500	5% BSA in 1X TBS-T	No
HA	Rat	Roche	11867423001	1:1000	5% BSA in 1X TBS-T	1X
FLAG	Mouse	Sigma-Aldrich	F3165	1:1000	5% BSA in 1X TBS-T	1X
pS127 YAP	Rabbit	Cell Signaling	4911	1:1000	5% BSA in 1X TBS-T	No
IRDye 800CW anti-Rat	Goat	LICOR	925-32219	1:10,000	5% Milk in 1X TBS-T	1X
IRDye 800CW anti-Mouse	Goat	LICOR	925-32210	1:10,000	5% Milk in 1X TBS-T	1X
IRDye 800CW anti-Rabbit	Goat	LICOR	926-32211	1:10,000	5% Milk in 1X TBS-T	1X

Luciferase assay

$3*10^5$ HEK293T cells were seeded in 12-well culture plates and transfected on the same day. 1µg of total DNA was transfected per well using Lipofectamine 2000 (Invitrogen) (1µg of DNA:2µL of Lipofectamine 2000) and empty pcDNA vector was used to normalize amount of DNA transfected per well. Plasmids and amount of DNA

transfected are indicated in **Table 2.5**. Cells were harvested three days post-transfection. Media was aspirated. Cells were washed with 1mL ice-cold Phosphate-buffered Saline (PBS), and PBS was aspirated. Cells were lysed with 150µL of Passive Lysis Buffer (Promega Corporation) at room temperature for 10 minutes while rocking. Luciferase signal was measured with the Dual-Glo Luciferase Assay (Promega Corporation) in accordance to the manufacturer's directions using a Synergy H1 hybrid reader (Biotek). Prism (GraphPad Software) was used to conduct statistical analysis of Luciferase Assay results. Luciferase signal was normalized to signal detected when only Renilla-Luciferase was transfected. Data is represented as signal relative to that detected by co-transfection of Gal4-UAS-Luciferase, Gal4-TEAD4, and YAP2. P-values were determined using a one-way ANOVA test.

Table 2.5: Plasmids transfected in luciferase reporter assay

Plasmid	DNA Transfected (ng) / Well
pGL4.31-Gal4-UAS-Luciferase	100
pCMX-Gal4-Tead4	50
pRL-SV40P-Renilla	10
pcDNA3CMV-Yap2	25
pcDNA3-Myc-Lats1	75
pcDNA3-HA-Mob1	75
pcDNA3-HA-Mst2	75
pcDNA3-HA-hSalvador	75

Results

Designing Lats1 truncated variants

We used secondary structure predictions, sequence conservation, and structural information to design a series of Lats1 variants with truncated N-termini. Most of the N-terminal region of Lats1 is predicted to be disordered by secondary structure predictions, and between Lats1 homologs, there is minimal sequence conservation (**Figure 2.2A**). Two X-ray structures of Mob1 bound to the MBD of Lats1 revealed that the MBD went from disordered to ordered at residues 635-638 (Ni et al., 2015; Kim et al., 2016). The structures match secondary sequence predictions as α-helix formation is predicted to start at residue 636. Using these constraints, we designed a series of Lats1 variants with truncated N-termini that should maintain binding to Mob1 and kinase activity (**Table 2.6**).

We designed five Lats1 variants with N-terminal truncations (**Table 2.6**). Two began with the residues that were purified for crystallization in the structures of Lats1 MBD bound to Mob1, 603 and 622 (Ni et al., 2015; Kim et al., 2016). The variant starting at residue 612 spanned the two starts of the Lats1 MBD purified for crystallization (Ni et al., 2015; Kim et al., 2016). The variant starting at 635 represented Lats1 MBD that maintains ordered secondary structure in both secondary sequence predictions and the two crystal structures of Lats1 MBD bound to Mob1. Last, we made a Lats1 variant that lacked the entire MBD to use as a negative control; the variant started at 713. Here, the Lats1 variants with truncated N-termini will be referred to by their starting residue with the Kavran Lab plasmid code indicated in brackets.

We used the same techniques to design a series of Lats1 variants with truncated C-termini. The hydrophobic motif within the C-terminus is highly conserved within not only LATS/NDR kinases but also the AGC kinase family (Pearce et al., 2010). Other than the hydrophobic motif, which is predicted to form a β-strand, most of the region C-terminal to the kinase domain is predicted to be disordered by secondary structure predictions. Also, between Lats1/2 homologs, there is minimal sequence conservation within the region C-terminal to the kinase domain (**Figure 2.2B**).

We designed six Lats1 variants with C-terminal truncations (**Table 2.6**). We made a Lats1 variant that ended at residue 1078, thus lacking T1079 to serve as a negative control when detecting kinase activity. Residue T1079 is necessary for Lats1 kinase activation (Chan et al., 2005). The variant terminating at residue 1085 conserves the C-terminal region until the end of the hydrophobic motif. The last four variants (terminating at residues 1092, 1100, 1109, and 1119) were designed to terminate further along the C-terminal tail where there is minimal sequence conservation and no predicted secondary structure. Here, the Lats1 variants with truncated C-termini will be referred to by their last residue with the Kavran Lab plasmid code indicated in brackets (**Table 2.6**).

Table 2.6: Lats1 N-terminal and C-terminal truncated variants

	Residues	Kavran Lab Code	Notes
N-Terminal Truncations	603 - 1130	FS	Lats1 MBD purified by Ni et al., 2015
	612 - 1130	GI	Intermediate between 603 [FS] and 635 [GJ]
	622 - 1130	GN	Lats1 MBD purified by Kim et al., 2016
	635 - 1130	GJ	Lats1 MBD predicted to maintain secondary structure
	713 - 1130	FZ	Negative control: truncation of entire Lats1 Mob1 binding domain
C-Terminal Truncations	1 - 1078	HE	Negative control: T1079 is truncated
	1 - 1085	HB	Preserves the hydrophobic motif
	1 - 1092	FW	Extension of C-terminal region beyond the hydrophic motif (unconserved and unstructured)
	1 - 1100	FV	Extends C-terminal region beyond the hydrophic motif (unconserved and unstructured)
	1 - 1109	FU	Extends C-terminal region beyond the hydrophic motif (unconserved and unstructured)
	1 - 1119	FT	Extends C-terminal region beyond the hydrophic motif (unconserved and unstructured)

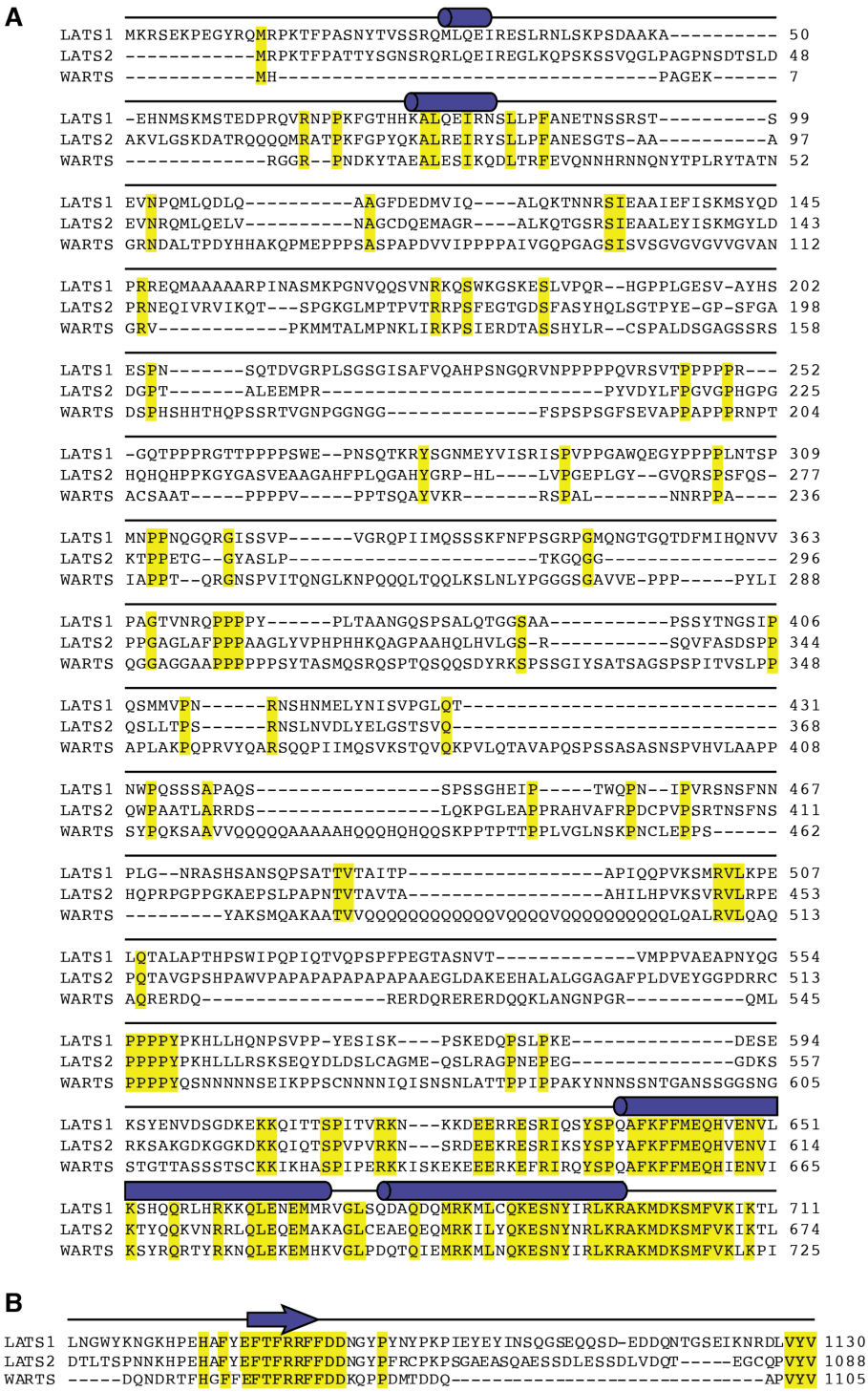

Figure 2.2: Analysis of the N-terminal and C-terminal regions of Lats1 kinase
A. Secondary sequence predictions and sequence alignment of region N-terminal to the kinase domain. Residues conserved between Lats1, Lats2, and Warts are highlighted in yellow (16% sequence identity). Cylinders represent α-helixes detected by secondary sequence predictions within the Lats1 N-terminus. **B.** Secondary sequence predictions and sequence alignment of region C-terminal to the kinase domain. Residues conserved between Lats1, Lats2, and Warts are highlighted in yellow (23% sequence identity). Arrow represents β-strand detected by secondary sequence predictions within the Lats1 C-terminus.

Validation of the minimal functional unit of Lats1

We planned to validate the function of the truncated Lats1 variants using three criteria. First, binding to Mob1 stimulates Lats1 substrate phosphorylation and autophosphorylation (Chan et al., 2005). We conducted a series of co-immunoprecipitations in HEK293 cells to examine complex formation between the Lats1 variants and Mob1. Second, Lats1 kinase is crucial for Hippo signaling as it mediates phosphorylation of YAP, the downstream target of Hippo signaling (Hao et al., 2008). We analyzed Lats1 kinase activity using two different experiments. HEK293 cells were transiently transfected with Mst2, Lats1, Mob1, and YAP. Phosphorylation of YAP was detected using Western blot analysis. Also, the luciferase reporter assay, which detects downstream Hippo pathway signaling, was used to compare kinase activity of the truncated Lats1 variants and wt Lats1. Third, Lats1 kinase activation requires phosphorylation of the hydrophobic motif by Mst2 and subsequent autophosphorylation of the activation loop (Chan et al., 2005). We aimed to transiently transfect HEK293 cells with the Lats1 variants, Mst2, and Mob1 and analyze the phosphorylation of those two residues using Western blot analysis.

Detecting complex formation of Lats1 and Mob1 in HEK293 cells

Truncated Lats1 variants and Mob1 were co-immunoprecipitated in HEK293 cells to analyze complex formation (**Figure 2.3**). As predicted, 713 [FZ] did not bind Mob1. 622 [GN] was the smallest Lats1 variant that bound Mob1 comparable to wt Lats1. Only one N-terminal variant other than 713 [FZ] did not bind Mob1 – 635 [GJ]. Truncating the

Lats1 C-terminus did not affect complex formation between the Lats1 variants and Mob1 (**Figure 2.3B**).

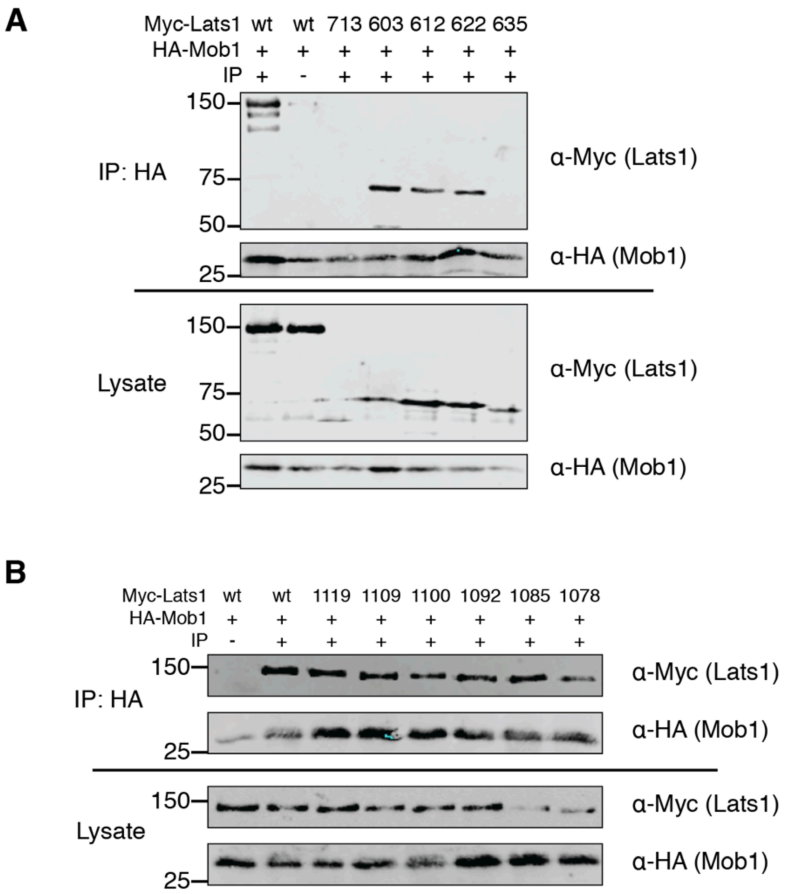

Figure 2.3: Testing complex formation between Lats1 truncated variants and Mob1 using co-immunoprecipitation

Either wt Myc-Lats1 or truncated Myc-Lats1 variants and HA-Mob1 were transiently transfected in HEK293 cells. Complex formation was analyzed by immunoprecipitation using α-HA antibody and detected using Western blot analysis. Fraction of cell lysate was probed using Western blot with epitope tags (Myc and HA) to detect protein expression. Co-immunoprecipitation of N-terminal truncated variants are shown in **A** and C-terminal truncated variants in **B**.

Analyzing substrate phosphorylation by truncated Lats1 kinase variants

We compared kinase activity of wt Lats1 and Lats1 truncated variants by detecting substrate phosphorylation using Western blot analysis. Mst2, Mob1, YAP, and Lats1 were transiently transfected into HEK293 cells, and phosphorylation of YAP was detected using Western blot analysis (**Figure 2.4**). We predicted that 1078 [HE] would not phosphorylate YAP as T1079, phosphorylation of which is necessary for Lats1 kinase activation, was truncated. We did not detect a discrete band to indicate phosphorylation of YAP by both 1078 [HE] and kd Lats1. We also detected minimal substrate phosphorylation by 713 [FZ] compared to wt Lats1. All other Lats1 truncated variants demonstrated substrate phosphorylation comparable to wt Lats1.

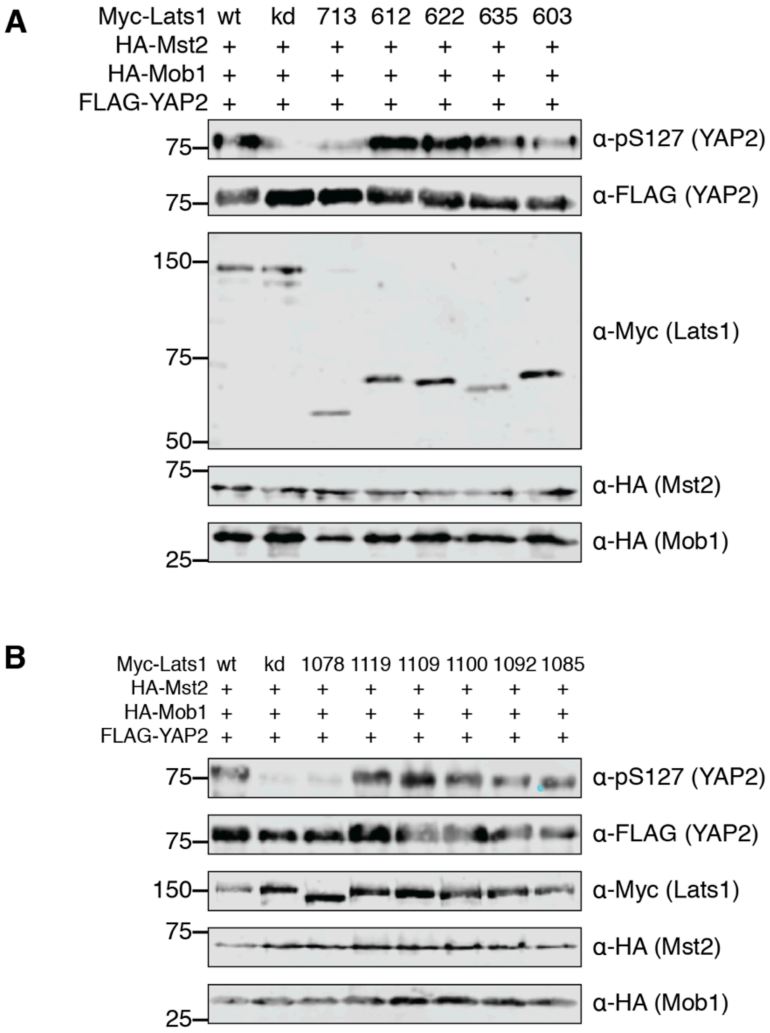

Figure 2.4: Analysis of substrate phosphorylation by truncated Lats1 variants using Western blot

HEK293 cells were transiently transfected with wt, kd, or truncated Myc-Lats1 variants, HA-Mst2, HA-Mob1, and FLAG-YAP2. Myc-Lats1 substrate phosphorylation was detected by Western blot analysis using YAP phospho-specific antibody (YAP - pS127). Immunoblots of Myc-Lats1, HA-Mst2, HA-Mob1, and FLAG-YAP2 expression are also shown. N-terminal truncated Myc-Lats1 variants are shown in **A.** and C-terminal truncated Myc-Lats1 variants in **B.**

Transient transfection of truncated Lats1 variants affect Hippo pathway function

Brendan Fowl conducted luciferase reporter assays in HEK293 cells to test Lats1 kinase activity as detected by Hippo pathway function (**Figure 2.5**). YAP phosphorylation by Lats1 kinase sequesters the transcriptional co-activator from the nucleus. Expression of luciferase indicates YAP localization to the nucleus. Thus, a decrease in luciferase expression is dependent upon phosphorylation of YAP and subsequent inhibition of YAP transcriptional co-activity. Transient transfection of the two variants that we designed to serve as negative controls for the phosphorylation of hydrophobic motif and Mob1 binding, 1078 [HE] and 713 [FZ] respectively, resulted in significantly increased activity status of YAP from wt Lats1. Transient transfection of all other Lats1 variants resulted in an insignificant change in luciferase activity when compared to wt Lats1.

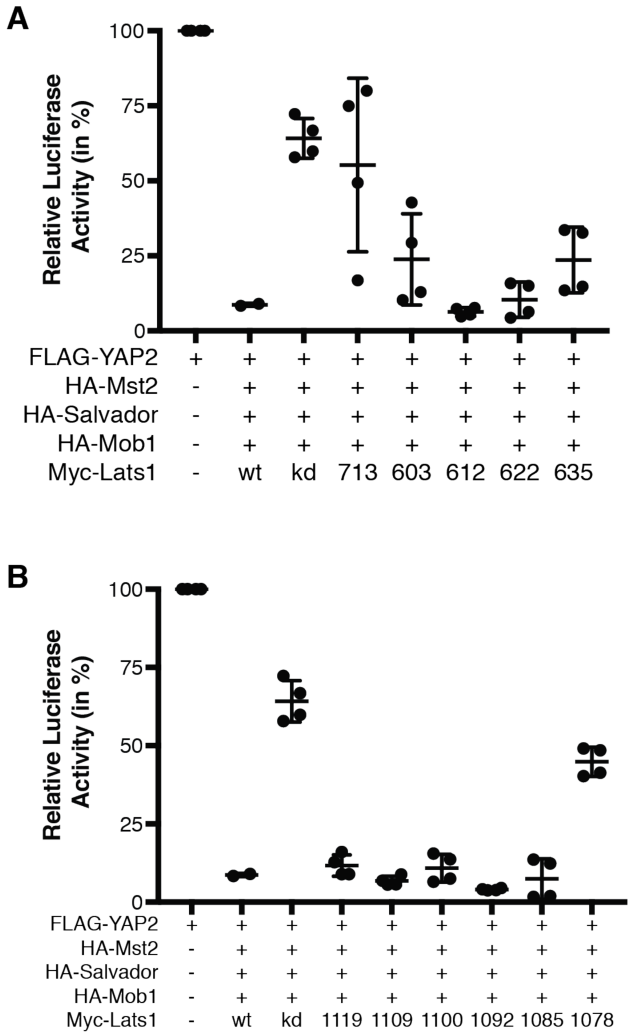

Figure 2.5: Validating kinase activity of Lats1 variants by detecting Hippo pathway function

The luciferase reporter assay was used to measure Lats1 suppression of YAP transcriptional co-activity in HEK293 cells. The fire-fly luciferase signal was normalized to the signal from renilla luciferase. The data was plotted as luciferase signal compared to luciferase signal from YAP2 (in %) and are from four measurements. Standard deviation and the mean are represented by error bars and horizontal bar, respectively. **A.** Comparing pathway function in cells transfected with N-terminal truncated Myc-Lats1 variants. P value between control and wt Lats1 is < 0.0001. P value between wt Lats1 and 713 [FZ] is 0.0060. P value between wt Lats1 and kd Lats1 is 0.0012. **B.** Comparing pathway function in cells transfected with C-terminal truncated Myc-Lats1 variants. P-value between wt Myc-Lats1 and control is <0.0001. P value between wt Lats1 and 1078 [HE] is < 0.0001. P value between wt Lats1 and kd Lats1 is < 0.0001.

Discussion

In the Kavran Lab, our goal is to purify Lats1 kinase and resolve the structure of Lats1 kinase using X-ray crystallography. Here, we aimed to isolate a minimal, functional unit of Lats1 that would maintain phosphorylation of the hydrophobic motif by Mst2, autophosphorylation of the activation loop, binding to Mob1, and substrate phosphorylation comparable to wt Lats1. We designed truncations of the N and C-termini of Lats1 to minimize the predicted disordered regions and experiments to validate the function of the truncated Lats1 variants. Thus far, we have isolated sections of the N and C-termini of Lats1 that preserve Lats1 binding to Mob1 and mediate comparable substrate phosphorylation and pathway function as wt Lats1.

We used secondary structure predictions and sequence conservation to design the N-terminal and C-terminal truncations of Lats1 (**Figure 2.1**). We also referred to previous structural analysis of Lats1 MBD to design N-terminal truncations of Lats1 that would mediate binding of Lats1 to Mob1 (Ni et al., 2015; Kim et al., 2016). The smallest Lats1 N-terminal truncated variant that binds Mob1 and maintains comparable kinase activity as wt Lats1 is 622 [GN], which encompasses the MBD purified by Kim et al. (Kim et al., 2016). The smallest Lats1 C-terminal truncated variant that binds Mob1 and maintains comparable kinase activity as wt Lats1 is 1085 [HB] that preserves the hydrophobic motif within the C-terminal tail.

We predicted that truncated Lats1 variants that cannot bind Mob1 would also have decreased kinase activity compared to wt Lats1 as Mob1 binding stimulates substrate phosphorylation by Lats1 (Chan et al., 2005). Although we did not detect complex formation between 635 [GJ] and Mob1, 635 [GJ] had comparable kinase

activity to wt Lats1 analyzed by substrate phosphorylation and pathway function. We knew that we could detect changes in Lats1 kinase activity resulting from inhibition of Lats1 binding to Mob1 as 713 [FZ] showed a significant difference in both pathway function and substrate phosphorylation when compared to wt Lats1. The difference in results on the function of 635 [GJ] may be attributed to decreased expression. Immunoblots of cell lysate from the co-immunoprecipitation and substrate phosphorylation experiments showed decreased 635 [GJ] expression that may have affected the capture of the 635 [GJ]:Mob1 complex using co-immunoprecipitation (**Figure 2.3A**). I plan to repeat co-immunoprecipitation of 635 [GJ] and Mob1 from cell lysate using more sensitive detection methods to determine whether 635 [GJ] and Mob1 form a protein:protein complex as suggested by the results from the luciferase reporter assay and the detection of substrate phosphorylation analyzed by Western blot.

The molecular role of Mob1 in the activation of Lats1 kinase

Introduction

Mob1 in the Hippo signaling pathway interacts with both kinases of the Hippo pathway core kinase cassette. Mob1 is phosphorylated by Mst1/2 kinase (Praskova et al., 2008). Multiple studies have demonstrated that phosphorylation of Mst1/2 enhances Mob1 binding to Lats1/2 kinase (Ni et al., 2015; Xiong et al., 2017). When Mob1 binds Lats1/2 kinase, both Lats1/2 autophosphorylation and substrate phosphorylation are stimulated (Bothos et al., 2005). Thus, the role of Mob1 in Hippo signaling is crucial as Mob1 stimulates Lats1/2 kinase activity resulting in phosphorylation of YAP, the downstream target of the Hippo tumor suppressor pathway (Hao et al., 2008). Here, we aim to elucidate the molecular role of Mob1 in the activation of Lats1 kinase.

Mob1 is comprised of two unique domains. The core domain is comprised of nine α-helices and two β-strands. The N-terminal extension (NTE) is a flexible region that associates with the core domain. The crystal structure of full-length, unphosphorylated Mob1 demonstrates two components that stabilize the interaction between the NTE and core domain (Kim et al., 2016) (**Figure 3.1**). First, a 4-turn α-helix in the NTE binds the core domain through electrostatic and hydrophobic interactions. Second, a β-strand in the NTE associates with a β-strand of the Mob1 core domain to form an antiparallel β-sheet.

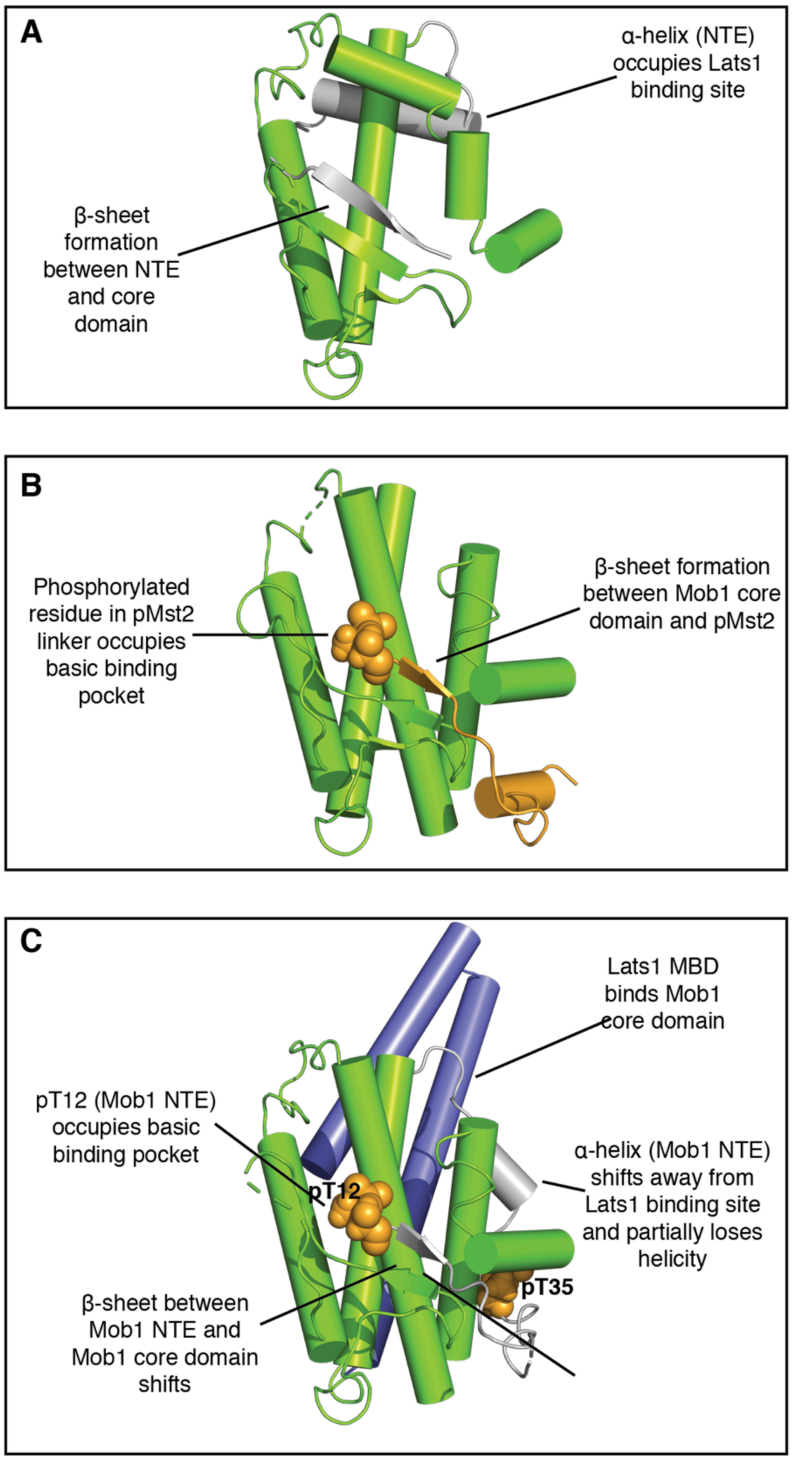

Figure 3.1: Mob1 N-terminal extension undergoes conformational change when phosphorylated by Mst2

A. Structure of full-length, unphosphorylated Mob1 (green) (Kim et al., 2016). The NTE (gray) associates with the Mob1 core domain (green). **B.** Structure of pMst2 (orange) phosphopeptide bound to unphosphorylated Mob1 (Ni et al., 2015). **C.** Structure of Lats1 MBD (blue) bound to phosphorylated Mob1 (pMob1). The residues phosphorylated by Mst2 (pT12 and pT35) are indicated in orange (Ni et al., 2015).

Upon phosphorylation, the NTE undergoes a conformational change as revealed by comparing the structures of full-length, unphosphorylated Mob1 and phosphorylated Mob1 bound to Lats1 MBD (Ni et al., 2015; Kim et al., 2016) (**Figure 3.1**). Mst2 phosphorylates two residues in the NTE, T12 and T35 (Praskova et al., 2008). T35 lies at the C-terminal end of the NTE 4-turn α-helix within a hydrophobic patch of the Mob1 core domain. Phosphorylation of T35 results in electrostatic repulsion and steric clash that contributes to the conformational change of the NTE – loss of partial helicity and the α-helix shifting away from the Mob1 core domain. Phosphorylated T12 can now occupy a phosphopeptide binding pocket comprised of basic amino acid residues within the Mob1 core domain. The movement of the NTE results in a shift of the β-sheet formed by the NTE and Mob1 core domain.

Three key domains comprise Mst2 kinase: a kinase domain and C-terminal SARAH dimerization domain that are connected by a long-flexible linker domain. Dimerization of Mst2 results in autophosphorylation of the activation loop within the kinase domain and subsequent autophosphorylation of various serine/threonine residues in the linker domain (Ni et al., 2013). Ni et al. demonstrated that Mob1 binds the phosphorylated linker domain of Mst2 as depicted by a crystal structure of unphosphorylated Mob1 bound to a phosphorylated Mst2 (pMst2) peptide (**Figure 3.1**) (Ni et al., 2015).

Phosphorylation induced conformational changes in Mob1 destabilize complex formation between Mob1 and pMst2 (Ni et al., 2015). First, pT12 of Mob1 and the phosphorylated residues of the Mst2 linker compete for the same phosphopeptide binding pocket within the Mob1 core domain. Second, both the NTE and pMst2 linker domain

associates with the same β-strand of the Mob1 core domain. pMob1 has lower binding affinity to pMst2 than unphosphorylated Mob1 that suggests phosphorylation induced conformational changes in Mob1 mediates release of Mob1 (Xiong et al., 2017).

Phosphorylation of Mob1 results in a conformational change in the NTE that relieves a steric block of the Lats1 binding site within the Mob1 core domain (Ni et al., 2015; Kim et al., 2016). In unphosphorylated Mob1, the 4-turn α-helix within the NTE occupies the Lats1 binding site in the Mob1 core domain. Xiong et al. demonstrated that the NTE of Mob1 and Lats1 MBD compete to bind the Mob1 core domain (Xiong et al., 2017). The importance of phosphorylation of T12 and T35 for Lats1 binding to Mob1 has been validated in different binding experiments completed with T12A/T35A Mob1 mutants (Praskova et al., 2008; Ni et al., 2015; Xiong et al., 2017). Thus, both structural and mutational analysis confirm phosphorylation of Mob1 results in a conformational change in the NTE that assists Lats1-Mob1 binding.

A recent study identified that Lats1 binding to Mob1 not only stimulate Lats1 kinase activity but also the phosphorylation of Lats1 by Mst2 (Ni et al., 2015). Hoa et al. observed that interrupting the Lats2-Mob1 binding interaction inhibits phosphorylation of Lats2 hydrophobic motif (Hoa et al., 2016). Ni et al. hypothesized that Mob1 mediates the recruitment of Mst2 and Lats1 resulting in stimulation of Lats1 hydrophobic motif phosphorylation because the pMst2 and Lats1 binding sites within the Mob1 core domain do not intersect. They isolated a ternary complex between Lats1 MBD, pMst2, and unphosphorylated Mob1 *in vitro* using gel filtration chromatography (Ni et al., 2015).

Although the structures of Mob1, mutational analysis, and reported binding affinities between Mob1, Lats1, and pMst2 give insight into the binding interactions that

mediate Hippo signaling, we have yet to fully resolve how Mob1 regulates Lats1 kinase activity. Here, we asked what the molecular role of Mob1 is in the activation of Lats1 kinase. Specifically, we analyzed the role of Mob1 in hydrophobic motif phosphorylation of Lats1 by Mst2, a necessary event for Lats1 kinase activation (Chan et al., 2005).

Table 3.1: Reported K_d between Mob1 core domain and Mob1 N-terminal extension

		Kd (uM)	Technique	Reference
Mob1A	Mob1 NTE Peptide (21 - 38)	>1000	Fluorescence Polarization Binding Assay	(Xiong et al., 2017)
Mob1A Core Domain (Δ 13)	Mob1 NTE Peptide (21 - 38)	>1000	Fluorescence Polarization Binding Assay	(Xiong et al., 2017)
Mob1A Core Domain (Δ 38)	Mob1 NTE Peptide (21 - 38)	570	Fluorescence Polarization Binding Assay	(Xiong et al., 2017)
Mob1A Core Domain (Δ 51)	Mob1 NTE Peptide (21 - 38)	350	Fluorescence Polarization Binding Assay	(Xiong et al., 2017)
pMob1A	Mob1 NTE Peptide (21 - 38)	210	Fluorescence Polarization Binding Assay	(Xiong et al., 2017)
Mob1A Core Domain (Δ 38)	Mob1A NTE T12 Peptide	N.D.	Fluorescence Polarization Binding Assay	(Xiong et al., 2017)
Mob1A Core Domain (Δ 38)	Mob1A NTE pT12 Peptide	318	Fluorescence Polarization Binding Assay	(Xiong et al., 2017)

Table 3.2: Reported K_d between NDR1 and Mob1

		Kd (uM)	Technique	Reference
NDR1 Mob1 Binding Domain (12 - 418)	Mob1A	26.3	Fluorescence Polarization Binding Assay	(Xiong et al., 2017)
NDR1 Mob1 Binding Domain (12 - 418)	pMob1A	2.5	Fluorescence Polarization Binding Assay	(Xiong et al., 2017)
NDR1 Mob1 Binding Domain (12 - 418)	Mob1A H24A Q25A	12.3	Fluorescence Polarization Binding Assay	(Xiong et al., 2017)
NDR1 Mob1 Binding Domain (12 - 418)	pMob1A H24A Q25A	2.6	Fluorescence Polarization Binding Assay	(Xiong et al., 2017)
NDR1 Mob1 Binding Domain (12 - 418)	Core Domain (Mob1 Δ 13)	26.3	Fluorescence Polarization Binding Assay	(Xiong et al., 2017)
NDR1 Mob1 Binding Domain (12 - 418)	Core Domain (pMob1 Δ 13)	1.6	Fluorescence Polarization Binding Assay	(Xiong et al., 2017)
NDR1 Mob1 Binding Domain (12 - 418)	Core Domain (Mob1 Δ 38)	9.6	Fluorescence Polarization Binding Assay	(Xiong et al., 2017)
NDR1 Mob1 Binding Domain (12 - 418)	Core Domain (pMob1 Δ 38)	8	Fluorescence Polarization Binding Assay	(Xiong et al., 2017)
NDR1 Mob1 Binding Domain (12 - 418)	Core Domain (Mob1 Δ 51)	51	Fluorescence Polarization Binding Assay	(Xiong et al., 2017)
NDR1 Mob1 Binding Domain (12 - 418)	Core Domain (pMob1 Δ 51)	35	Fluorescence Polarization Binding Assay	(Xiong et al., 2017)
NDR1 Mob1 Binding Domain (12 - 418)	Mob1A	22.3	Microscale Thermophoresis Binding Analysis	(Xiong et al., 2017)
NDR1 Mob1 Binding Domain (12 - 418)	pMob1A	2.6	Microscale Thermophoresis Binding Analysis	(Xiong et al., 2017)
NDR1 Mob1 Binding Domain (12 - 418)	pMob1A T12 - 353	0.7	Microscale Thermophoresis Binding Analysis	(Xiong et al., 2017)
NDR1 Mob1 Binding Domain (12 - 418)	pMob1A T35A	5	Microscale Thermophoresis Binding Analysis	(Xiong et al., 2017)
NDR1 Mob1 Binding Domain (12 - 418)	pMob1A T12A	1.6	Microscale Thermophoresis Binding Analysis	(Xiong et al., 2017)

Table 3.3: Reported K_d between Mob1A and Mst2

		Kd (uM)	Technique	Reference
Mob1A	Mst2 Phosphopeptide (Residues 371 - 401)	0.119	Isothermal Titration Calorimetry	(Ni et al., 2015)
Mob1A	Mst2 Δ Linker (9 - 313; 428 - 491)	0.23	Isothermal Titration Calorimetry	(Ni et al., 2015)
Mob1A	Mst2 Linker (pT353)	0.28	Binding Assay	(Xiong et al., 2017)
pMob1A	Mst2 Linker (pT353)	13.3	Binding Assay	(Xiong et al., 2017)
Mob1A	Mst2 Linker (pT367)	0.68	Binding Assay	(Xiong et al., 2017)
pMob1A	Mst2 Linker (pT367)	15.3	Binding Assay	(Xiong et al., 2017)
Mob1A T35A	Mst2 Phosphopeptide	0.53	Fluorescence Polarization Binding Assay	(Xiong et al., 2017)
pMob1A T35A	Mst2 Phosphopeptide	0.81	Fluorescence Polarization Binding Assay	(Xiong et al., 2017)
Mob1A T12A	Mst2 Phosphopeptide	0.51	Fluorescence Polarization Binding Assay	(Xiong et al., 2017)
pMob1A T12A	Mst2 Phosphopeptide	2.9	Fluorescence Polarization Binding Assay	(Xiong et al., 2017)
Mob1A	Mst2 pT353 Peptide	0.28	Binding Assay	(Couzen et al., 2017)
Mob1A	Mst2 T353 Peptide	N.D.	Binding Assay	(Couzen et al., 2017)
Mob1A	Mst2 pT367 Peptide	0.68	Binding Assay	(Couzen et al., 2017)
Mob1A	Mst2 T367 Peptide	N.D.	Binding Assay	(Couzen et al., 2017)
Mob1A K153A, R154A, R157A	Mst2 pT353 Peptide	N.D.	Fluorescence Polarization Binding Assay	(Couzen et al., 2017)
Mob1A	Mst2 pT353 Peptide	0.31	Binding Assay	(Couzen et al., 2017)
Mob1A K153A, R154A, R157A	Mst2 pT367 Peptide	N.D.	Fluorescence Polarization Binding Assay	(Couzen et al., 2017)
Mob1A	Mst2 pT367 Peptide	0.58	Binding Assay	(Couzen et al., 2017)
Mob1A	Mst2 T329/T340 15mer Peptide	N.D.	Fluorescence Polarization Binding Assay	(Couzen et al., 2017)
Mob1A	Mst2 pT329/T340 15mer Peptide	47	Fluorescence Polarization Binding Assay	(Couzen et al., 2017)
Mob1A	Mst2 T329/pT340 15mer Peptide	66	Fluorescence Polarization Binding Assay	(Couzen et al., 2017)
Mob1A	Mst2 pT329/pT340 15mer Peptide	49	Fluorescence Polarization Binding Assay	(Couzen et al., 2017)
Mob1A	Mst2 T380/T387 15mer Peptide	N.D.	Fluorescence Polarization Binding Assay	(Couzen et al., 2017)
Mob1A	Mst2 T380/pT387 15mer Peptide	N.D.	Fluorescence Polarization Binding Assay	(Couzen et al., 2017)
Mob1A	Mst2 pT380/T387 15mer Peptide	186	Fluorescence Polarization Binding Assay	(Couzen et al., 2017)
Mob1A	Mst2 pT380/pT387 15mer Peptide	95	Fluorescence Polarization Binding Assay	(Couzen et al., 2017)

Materials and Methods

Transient transfection of HEK293 cells

HEK293T cells were cultured in DMEM medium (Gibco) supplemented with 5% FBEssence (VWR) and 2mM Glutamine (Thermo Fischer) and grown at 37℃ and 5% CO_2. $0.6*10^6$ HEK293T cells were seeded in 6-well plate and transiently transfected one day later using polyethylenimine hydrochloride transfection reagent (PEI Max, Polysciences Inc.) at a ratio of 3µl of PEI Max to 1µg of DNA. The pcDNA plasmids transfected are indicated in **Table 3.4**. 48 hours after transfection, cell medium was aspirated, and cells were washed with 1mL ice-cold phosphate-buffered saline (PBS). PBS was aspirated, and cells were incubated with ice-cold immunoprecipitation buffer (IP buffer) (20mM Tris pH 8.0, 150mM NaCl, 1% Nonidet P-40 (NP-40), and 10% glycerol) supplemented with 50mM NaF, 1mM Na_3VO_4, 0.5mM PMSF, and Pierce Universal Nuclease (Thermo Scientific, 1:10,000) while rocking for 30 minutes at 4℃. Cell lysates were clarified by centrifugation at 23,000rpm for 10 minutes at 4℃. The total protein concentration in the lysate of each sample was quantified using the Pierce BCA protein assay kit (Thermo Scientific).

Table 3.4: pcDNA plasmids transfected in HEK293 cells

Protein	Epitope Tag	Vector	Kavran Lab Code	DNA Transfected (ng)/Well
Lats1	Myc	pcDNA	97	1200
Mob1	FLAG	pcDNA	JA	400
Mst2	HA	pcDNA	94	400

Western blot analysis

Samples were resolved on 10 or 15% sodium dodecyl sulfate-polyacrylamide gel electrophoresis (SDS-PAGE) and transferred to nitrocellulose membranes (0.45µm) using the Trans-Blot Turbo Transfer System (Bio-Rad). Membranes were blocked in 5% skimmed milk powder in TBS (20mM Tris pH 7.6 and 150mM NaCl) for 30 minutes at room temperature. Membranes were probed with primary antibodies overnight at 4°C (**Table 3.5**). Membranes were washed three times with TBS-T (20mM Tris pH 7.6, 150mM NaCl, and 0.1% Tween 20) for 5 minutes. Then, membranes were incubated with fluorophore-conjugated secondary antibodies for 1 hour at room temperature. The membranes were washed three times with TBS-T for 5 minutes (**Table 3.5**). Blots were scanned on an Odyssey Infrared Imaging System (LI-COR) and analyzed using ImageStudio software (LI-COR). Band intensities were quantified using Image Studio (LI-COR), and Prism (GraphPad Software) was used to conduct statistical analysis.

Table 3.5: Antibodies used in Western blot analysis

Antibody	Host	Source	Reference	Dilution	Dilution Buffer	Repeated Use of Antibody?
c-Myc (9E10)	Mouse	Santa Cruz	sc-40	1:500	5% BSA in 1X TBS-T	No
HA	Rat	Roche	11867423001	1:1000	5% BSA in 1X TBS-T	1X
FLAG	Mouse	Sigma-Aldrich	F3165	1:1000	5% BSA in 1X TBS-T	1X
pT1079 Lats1	Rabbit	Cell Signaling	8654	1:1000	5% BSA in 1X TBS-T	No
IRDye 800CW anti-Rat	Goat	LICOR	925-32219	1:10,000	5% Milk in 1X TBS-T	1X
IRDye 800CW anti-Mouse	Goat	LICOR	925-32210	1:10,000	5% Milk in 1X TBS-T	1X
IRDye 800CW anti-Rabbit	Goat	LICOR	926-32211	1:10,000	5% Milk in 1X TBS-T	1X

Cloning Lats1 Mob1 binding domain

Residues 635-698 of Lats1 were cloned into a pSat-L vector downstream of a hexahistidine and SUMO tag using LIC cloning that was confirmed by DNA sequencing.

Purification of Lats1 Mob1 binding domain

Transformed T7 Express cells (New England BioLabs) were grown in 8L of TB media at 37°C. Cells were induced using 0.5mM IPTG at 1.7 OD_{600}. Following induction, cells were grown at 37°C for three hours.

Cells were resuspended in 150mL lysis buffer (50mM Tris pH 8.0, 800mM NaCl, and 10% glycerol) supplemented with protease inhibitor cocktail (Sigma-Aldrich). Cells were lysed using the micro-fluidizer. Lysate was clarified by centrifugation at 23,000rpm at 4°C for 30 minutes. 5mM ATP and 10mM $MgCl_2$ was added to supernatant. Supernatant was loaded onto 10mL column volume (CV) of Profinity-IMAC resin (Bio-Rad) and incubated for 1 hour at 4°C. Resin was collected by centrifugation at 1000rpm for 5 minutes at 4°C. Resin was washed in batch twice with 5CV of lysis buffer and three times with 5CV of lysis buffer supplemented with 10mM Imidazole. Lats1 MBD was eluted in 50mM Tris pH 8.0, 100mM NaCl, 5% glycerol, 5mM ATP, 10mM $MgCl_2$, and 125mM Imidazole. Lats1 MBD was incubated in 1:10 SENP (ratio of concentration of protein) for 1 hour at room temperature (Malakhov et al., 2004). Lats1 MBD was diluted with 20mM Tris pH 8.0 and 5% glycerol to lower the concentration of NaCl to 50mM and loaded onto a 5mL CV Hi Trap SP column (GE Healthcare). Lats1 MBD was eluted using an increasing NaCl concentration gradient. Fractions with Lats1 MBD were pooled,

and protein was clarified by centrifugation at 23,000rpm for 30 minutes at 4°C. Supernatant was diluted with 20mM HEPES pH 8.0 and 5% glycerol to lower the NaCl concentration to 50mM and loaded onto a 6mL CV Resource S cation exchange chromatography column (GE Healthcare). Lats1 MBD was eluted using an increasing NaCl concentration gradient. Fractions containing Lats1 MBD were pooled, and glycerol was added to store Lats1 MBD in 10% glycerol. Lats1 MBD was concentrated to 3.2mg/mL and flash frozen in liquid nitrogen.

Results

Co-transfection of Mob1 with Mst2 and Lats1 stimulates phosphorylation of Lats1 hydrophobic motif

We transiently transfected Mst2, Lats1, and Mob1 in HEK293 cells to analyze the phosphorylation of Lats1 hydrophobic motif using Western blot analysis (**Figure 3.2**). We replicated the experiment three times and found that Mob1 stimulates phosphorylation of Lats1 by Mst2. This result is in agreement with a previous study that also analyzed the effect of Mob1 in Lats1 kinase activation (Ni et al., 2015).

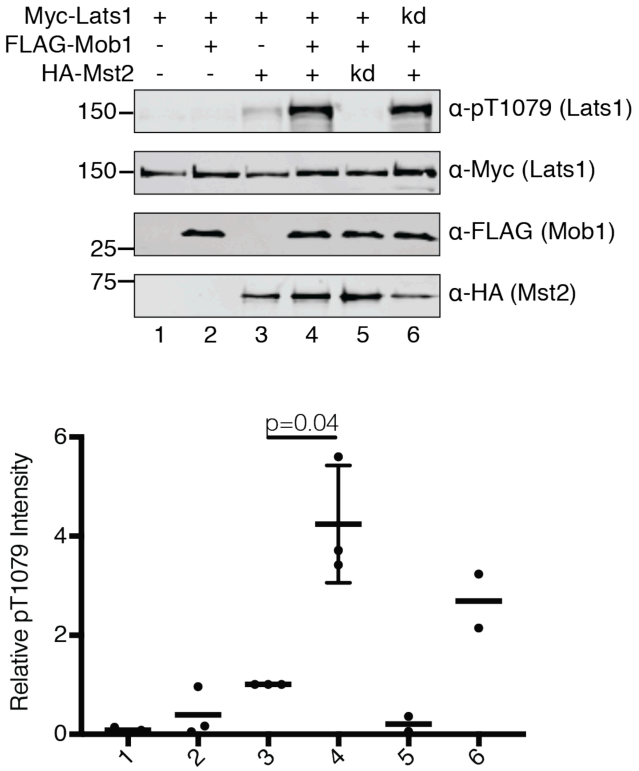

Figure 3.2: Mob1 stimulates Lats1 hydrophobic motif phosphorylation by Mst2
HEK293 cells co-transfected with indicated plasmids. Phosphorylation of Lats1 hydrophobic motif (pT1079 Lats1) and expression of Myc-Lats1, FLAG-Mob1, and HA-Mst2 were analyzed using Western blot. Representative blots from one experiment (top) and a scatterplot of replicates (bottom) are shown. Measurement of pT1079 Lats1 intensity was normalized to total Myc-Lats1 intensity. Data are plotted as normalized pT1079 signal compared to that from co-transfection of Lats1 and Mst2 (Lane 3). The P value between Mst2 and Lats1 co-transfection (Lane 3) and Mst2, Lats1, and Mob1 co-transfection (Lane 4) is 0.04.

Isolating the ternary complex *in vitro*

We aim to isolate the ternary complex *in vitro* using a series of pull-down experiments and analyze whether the phosphorylation state of Mob1 affects complex formation (**Figure 3.3**). We plan to purify Lats1 MBD, Mob1 both phosphorylated and unphosphorylated, and pMst2 to input in the pull-down experiment. By purifying both phosphorylated and unphosphorylated Mob1 for use in the pull-down experiment, we will be able to determine whether the phosphorylation state of Mob1 affects ternary complex formation.

We referenced previously conducted binding analysis to design proper negative and positive controls for the pull-down experiment as the proteins within the ternary complex – Lats1, Mob1, and Mst2 – have binding interactions independent of the formation of the ternary complex. Mst2 and Mob1 as well as Mob1 and Lats1 form complexes (Ni et al., 2015). However, Mst2 and Lats1, when co-expressed in cells, do not form a complex (Chan et al., 2005). First, we will confirm the Lats1-Mob1 and pMst2-Mob1 binding interactions. Then, we will validate that Lats1 MBD and pMst2 do not form a complex *in vitro*. With the establishment of these controls, we plan to couple Lats1 MBD to resin and detect ternary complex formation by analyzing pull-down of pMst2. If pMst2 is detected in the pull-down experiment, it will be a result of ternary complex formation rather than an independent binding interaction between pMst2 and Lats1 MBD. A representation of this experiment is demonstrated in **Figure 3.3**.

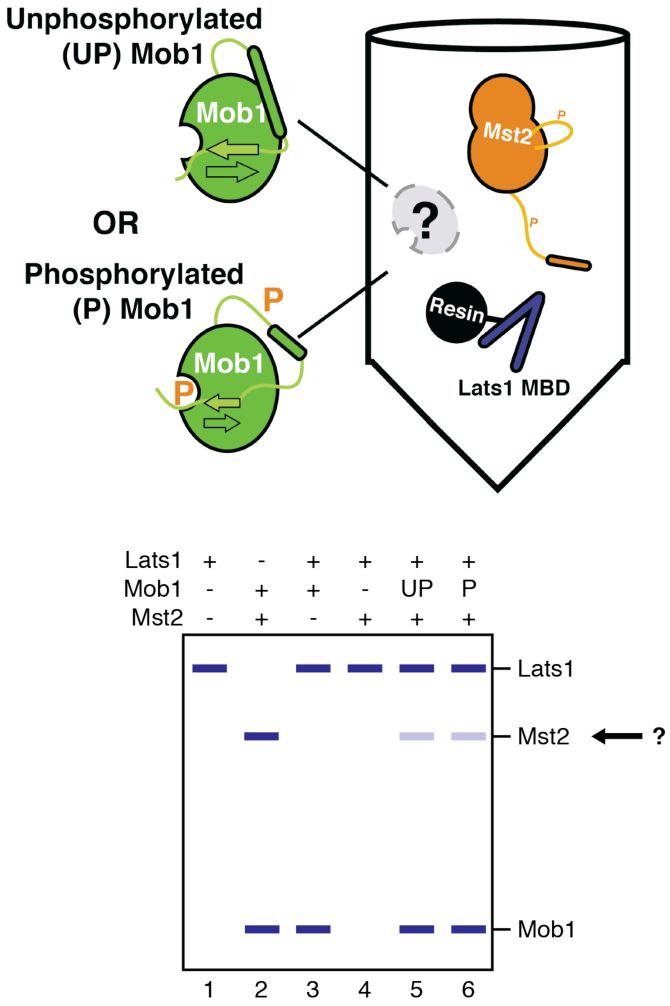

Figure 3.3: Pull-down of Lats1-Mob1-Mst2 ternary complex *in vitro*
A schematic of the pull-down experiment is shown. Lats1 MBD, Mst2, and both phosphorylated and unphosphorylated Mob1 will be purified *in vitro*. Then, pull-down experiments will be conducted to determine whether we can isolate ternary complex formation. Also, by inputting either phosphorylated or unphosphorylated Mob1 in the pull-down, we will be able to detect whether the phosphorylation state of Mob1 affects ternary complex formation.

Purification of Lats1 Mob1 binding domain

We expressed Lats1 MBD with a H_6SUMO affinity tag. Initial lysis conditions resulted in protein degradation and low solubility of protein (**Figure 3.4A**). We used different conditions to express H_6SUMO-Lats1 MBD and lyse cells following harvest. Shortening expression times from 20°C overnight to 37°C for 3 hours resulted in increased expression. We increased the ionic strength of the lysis buffer from 400mM to 800mM NaCl, which we reasoned would stabilize the basic surface of Lats1 MBD, to improve solubility. We also increased glycerol content from 5% to 10%. H_6SUMO-Lats1 MBD was soluble in the improved lysis buffer (**Figure 3.4B**).

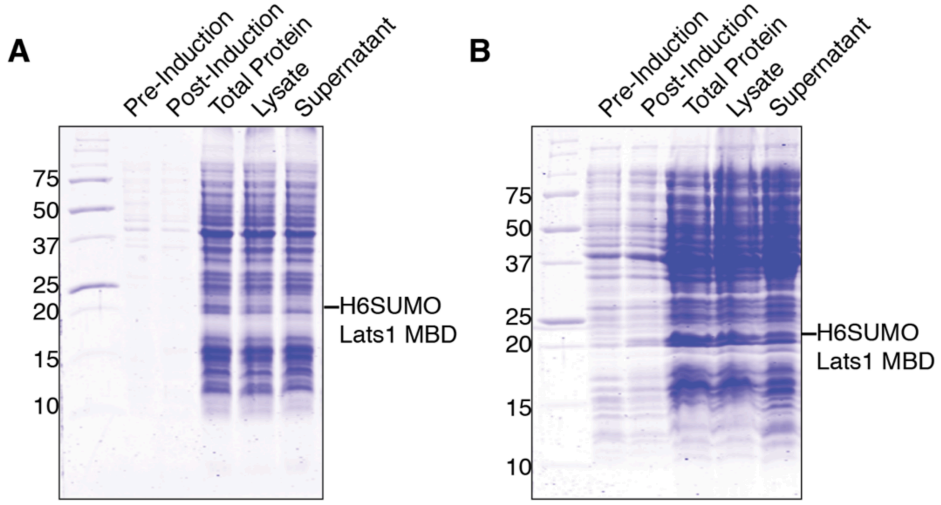

Figure 3.4: Methods to increase the solubility and expression of Lats1 Mob1 binding domain

A. Transformed T7 Express cells were grown in 8L of LB at 20°C overnight post-induction. Cells were lysed in 50mM Tris pH 8, 400mM NaCl, and 5% glycerol. Protein expression and solubility were analyzed by Coomassie stained SDS-Page gel. There was significant loss of H_6SUMO-Lats1 MBD solubility following clarification of cell lysate. **B.** Transformed T7 Express cells were grown in 8L of TB at 37°C for 3 hours post-induction. Cells were lysed in 50mM Tris pH 8, 800mM NaCl, and 10% glycerol. Protein expression and solubility were analyzed by Coomassie stained SDS-Page gel. H_6SUMO-Lats1 MBD remained soluble following clarification of cell lysate.

We isolated Lats1 MBD using affinity chromatography and cleaved the H_6SUMO tag by adding SENP (Malakhov et al., 2004). Lats1 MBD was further purified by cation exchange chromatography. During purification, monitoring absorbance at 280nm is not useful for Lats1 MBD as it does not contain any tryptophans. Chromatograms therefore better report on the presence of contaminants. During cation exchange chromatography, we found that the absorbance peaks were not representative of the elution peak of Lats1 MBD as the presence of other contaminants would overwhelm the absorbance signal. Thus, we relied on monitoring Lats1-MBD purification using Coomassie stained SDS PAGE (**Figure 3.5**).

Care must be taken when transferring the protein into a low salt buffer before loading onto the cation exchange chromatography column. When protein was diluted to 100mM NaCl prior to loading onto the column, Lats1 MBD was present in the flow-through and did not completely bind the cation exchange chromatography column (**Figure 3.5**). However, when protein was diluted to 50mM NaCl prior to loading onto the column, Lats1 MBD was not present in the flow-through fractions (**Figure 3.6**). Although higher NaCl concentrations improved solubility of Lats1 MBD in cell lysate, higher NaCl concentrations prevented Lats1 MBD to bind to the cation exchange chromatography column.

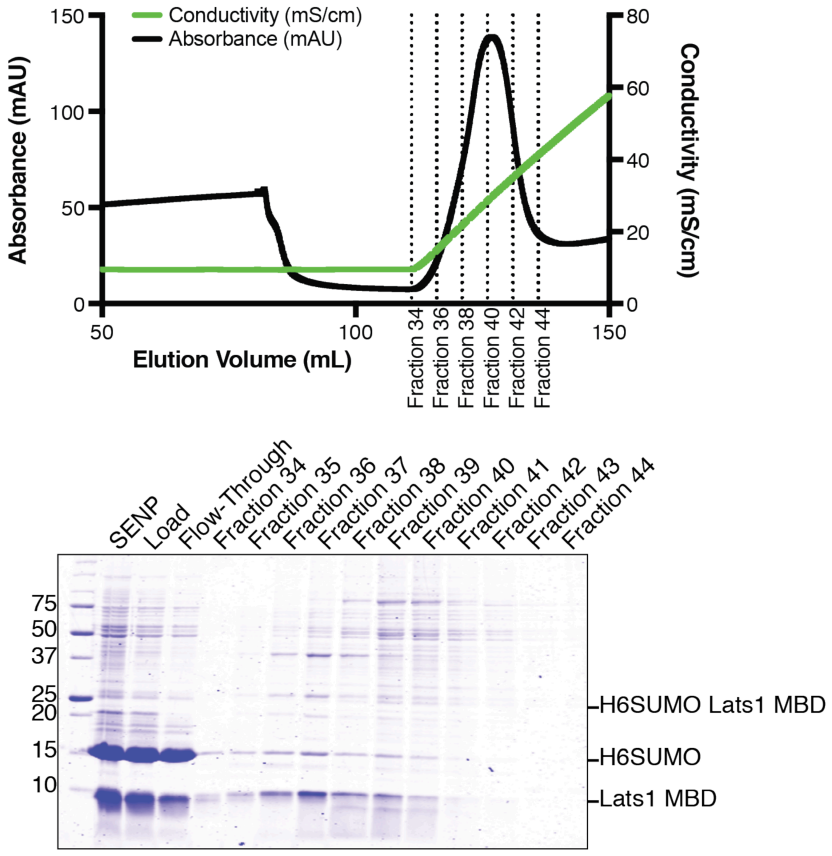

Figure 3.5: Limited binding of Lats1 Mob1 binding domain to the cation exchange chromatography column at 100mM NaCl

Chromatogram of cation exchange and accompanying Coomassie stained SDS-Page are displayed. H_6SUMO-Lats1 MBD was isolated first using IMAC. Then, the affinity tag was cleaved (SENP). Prior to loading onto the cation exchange chromatography column, protein was diluted to a final concentration of 100mM NaCl. Lats1 MBD was present in the flow-through and eluted in fractions 35 – 40.

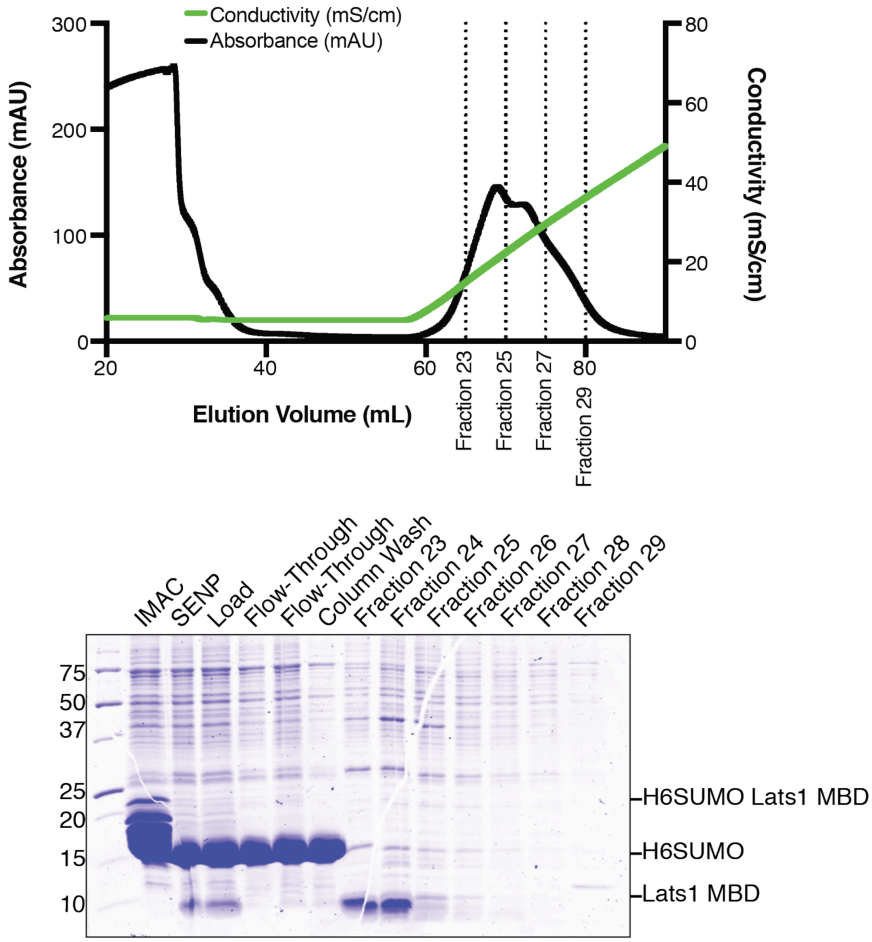

Figure 3.6: Lats1 Mob1 binding domain binds the cation exchange chromatography column at 50mM NaCl

Chromatogram of cation exchange and accompanying Coomassie stained SDS-Page are displayed. H_6SUMO-Lats1 MBD was isolated first using IMAC (IMAC). Then, the affinity tag was cleaved, and protein clarified (SENP). Prior to loading onto the cation exchange chromatography column, protein was diluted to a final concentration of 50mM NaCl. Lats1 MBD was not present in the flow-through fractions and eluted in fractions 23 and 24.

Gel filtration chromatography was used to further isolate Lats1-MBD (**Figure 3.7**). Initially, Lats1-MBD was isolated using gel filtration chromatography on a HiLoad 16/600 Superdex 75 size exclusion column (GE Healthcare) equilibrated in 20mM Tris pH 8.0, 100mM NaCl, and 5% glycerol. However, Lats1 MBD did not elute at the predicted volume. In fact, Lats1 MBD eluted after the entire volume of the column. We hypothesized that Lats1 MBD associates with the resin of the gel filtration column. Next, we loaded a fraction of Lats1 MBD from the initial gel filtration chromatography purification onto a Superdex 75 10/300GL gel filtration chromatography column equilibrated in 400mM NaCl to minimize any interactions between Lats1 MBD and resin. The elution profile of Lats1 MBD in high salt matched the predicted elution volume for a protein of that size.

We decided to repeat the elution conditions in the second gel filtration chromatography purification to a larger-scale purification of Lats1 MBD (**Figure 3.8**). We loaded Lats1 MBD on a Hi Load 26/600 Superdex 75 size exclusion column (GE Healthcare) equilibrated in 400mM NaCl following IMAC and cation exchange chromatography purification. However, we found that Lats1 MBD interacted with the column again. We concluded that Lats1 MBD associates with resin of Hi Load Superdex gel filtration chromatography columns despite increasing NaCl concentration during protein elution.

We could not use the Superdex 75 10/300GL gel filtration chromatography column due to volume constraints for future, large-scale purifications and decided to replace gel filtration chromatography with a second cation exchange chromatography

purification. We successfully separated Lats1 MBD from contaminants using the Resource S cation exchange chromatography column (**Figure 3.9**).

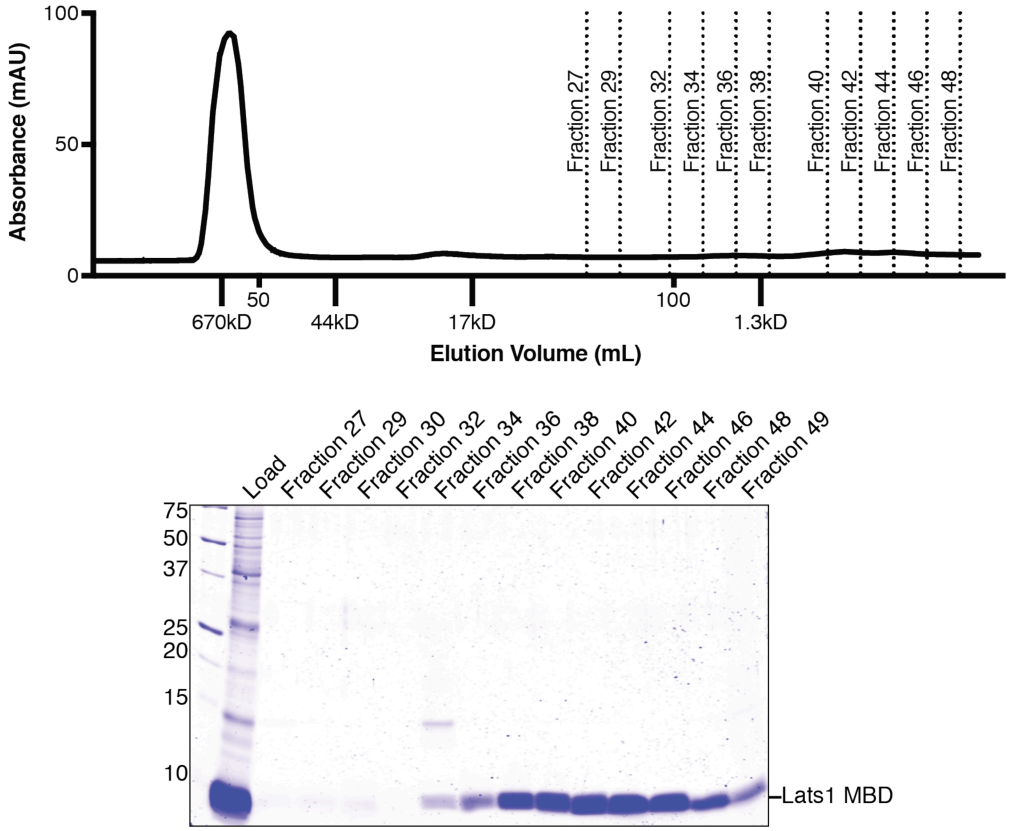

Figure 3.7: Lats1 Mob1 binding domain interacts with the gel filtration chromatography column

Chromatogram of gel filtration and accompanying Coomassie stained SDS-Page are displayed. Lat1 MBD was resolved using the HiLoad 16/600 Superdex 75 size exclusion column equilibrated in 20mM Tris pH 8.0, 100mM NaCl, 5mM BME, and 5% glycerol. Elution peaks of molecular weight standards previously fractionated using gel filtration chromatography are marked on the X-axis.

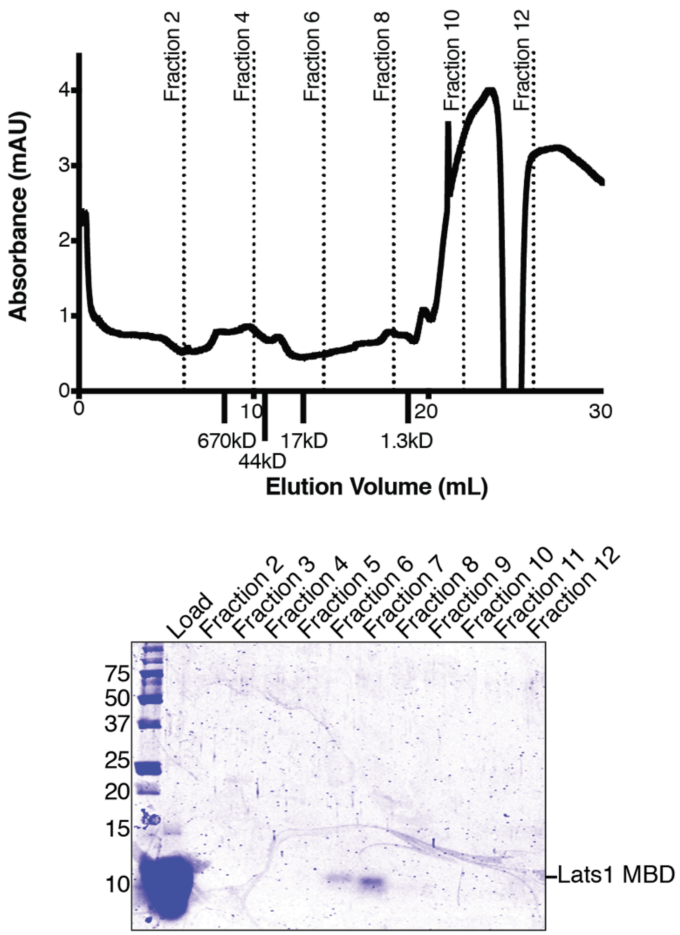

Figure 3.8: Increasing NaCl concentration minimizes Lats1 Mob1 binding domain interaction with resin of Superdex 75 10/300GL gel filtration chromatography column
Chromatogram of gel filtration and accompanying Coomassie stained SDS-Page are displayed. Lats1 MBD was loaded onto Superdex 75 10/300GL gel filtration chromatography column equilibrated in 20mM Tris pH 8.0, 400mM NaCl, 5mM BME, and 5% glycerol to see whether interaction of Lats1 MBD and resin of gel filtration column could be disrupted. Elution peaks of molecular weight standards previously resolved using Superdex 75 10/300GL gel filtration chromatography column are indicated on the X-axis. Lats1 MBD eluted in fractions 6 and 7.

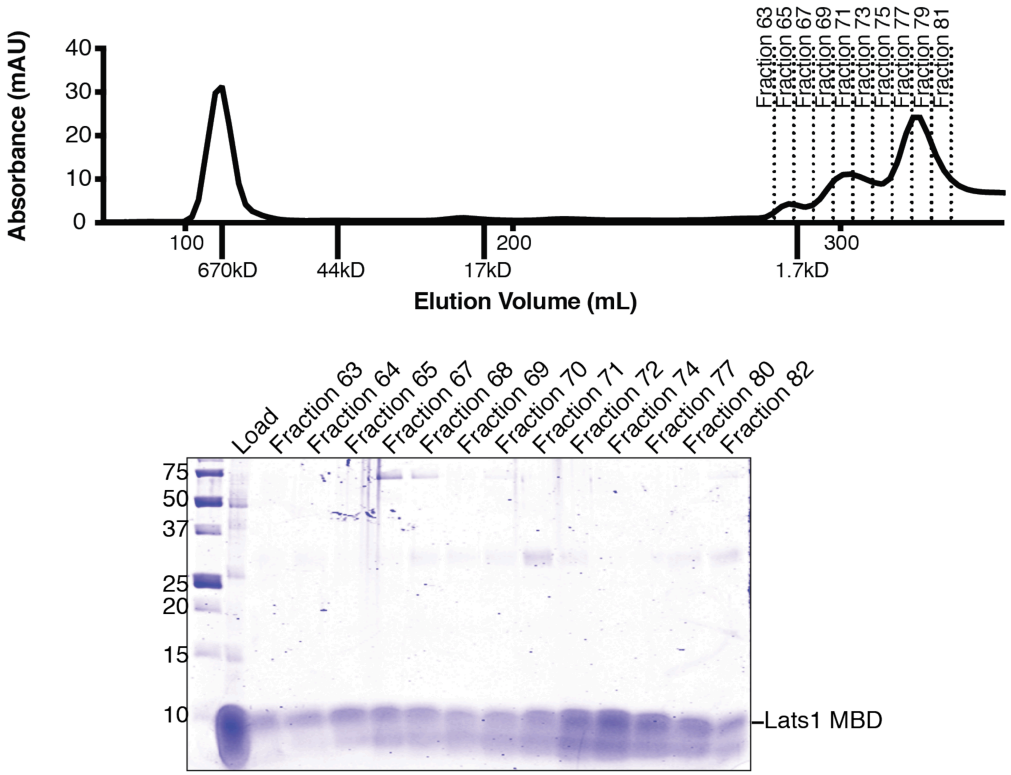

Figure 3.9: Increasing NaCl concentration does not disrupt the interaction between Lats1 Mob1 binding domain and HiLoad Superdex gel filtration chromatography columns
Chromatogram of gel filtration and accompanying Coomassie stained SDS-Page are displayed. Lats1 MBD was loaded onto HiLoad 26/600 Superdex 75 size exclusion column equilibrated with 10mM HEPES pH 8.0, 400mM NaCl, 5mM BME, and 5% glycerol to mimic the second gel filtration chromatography elution conditions (**Figure 3.8**). The elution peaks of molecular weight standards previously resolved using gel filtration chromatography are marked on the X-axis. Lats1 MBD, again, interacted with the resin of the gel filtration chromatography column.

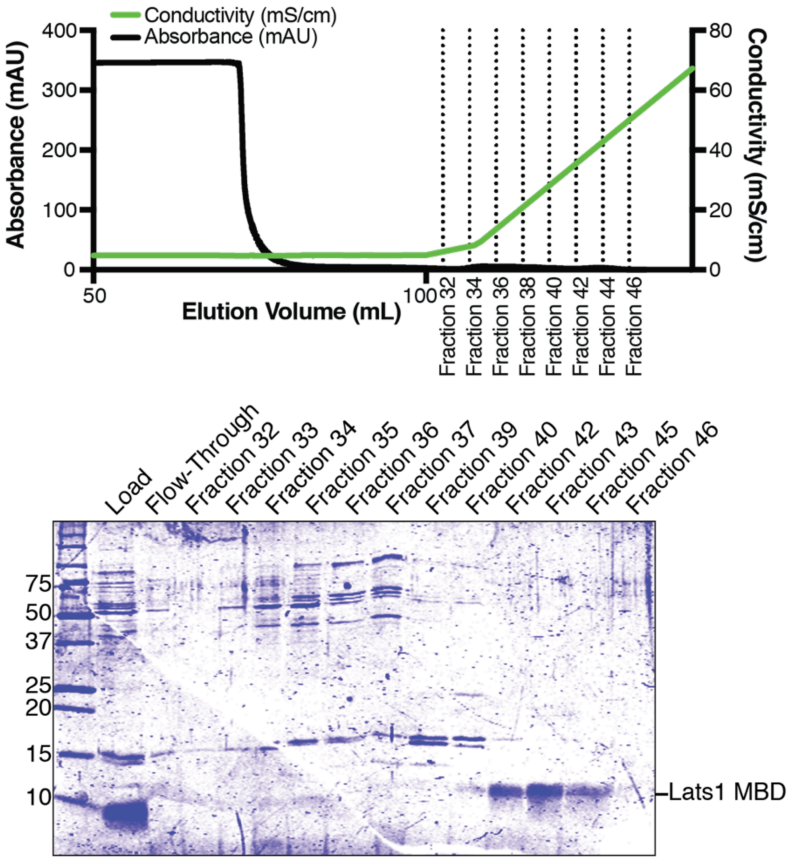

Figure 3.10: Substituting gel filtration chromatography with cation exchange chromatography results in complete isolation of Lats1 Mob1 binding domain
Chromatogram of cation exchange and accompanying Coomassie stained SDS-Page are displayed. Use of gel filtration chromatography for isolation of Lats1 MBD in large-scale purification was unsuccessful as Lats1 MBD interacts with resin of the gel filtration chromatography column. Lats1 MBD was purified using the Resource S cation exchange chromatography column to see if Lats1 MBD could be separated from contaminants without the use of gel filtration chromatography. Lats1 MBD eluted in fractions 42 – 45.

Discussion

Three components comprise Lats1 kinase activation and stimulation of Lats1 kinase activity: phosphorylation of T1079 within the hydrophobic motif by Mst2, autophosphorylation of S909, and binding to Mob1, a co-activator (Chan et al., 2005; Hergovich, Schmitz & Hemmings, 2006). Here, we aim to elucidate the molecular role of Mob1 in Lats1 kinase activation. We find that Mob1 co-expression with Mst2 and Lats1 stimulates phosphorylation of Lats1 hydrophobic motif by Mst2 in concordance with previous studies (Ni et al., 2015; Hoa et al., 2016).

Ni et al. hypothesized that Mob1 mediates the formation of a ternary complex between Lats1, pMst2, and Mob1 that results in stimulation of Lats1 phosphorylation by Mst2. Although the ternary complex has been observed *in vitro*, we aim to further validate that ternary complex formation mediates stimulation of Lats1 hydrophobic motif phosphorylation by Mst2 in HEK293 cells. We plan to interrupt both the Mob1-Mst2 and Mob1-Lats1 binding interactions in HEK293 cells and analyze Lats1 pT1079 phosphorylation using Western blot analysis. Mutating the basic amino acid residues (R697A, R694A, R657A, R660A, and S690A) within the Lats1 MBD inhibits Mob1 binding (Ni et al., 2015). Also, as previously mentioned, T12A/T35A Mob1 mutants also bind Lats1 MBD less than wt Mob1 (Praskova et al., 2008; Ni et al., 2015; Xiong et al., 2017). The Mob1 and Mst2 binding interaction is also inhibited with mutations of the basic amino acid residues (K153A, R154A, and R157A) that comprise the phosphopeptide binding pocket within the Mob1 core domain (Couzen et al., 2017). We will confirm that the mutations disrupt only the binding interaction of interest using co-immunoprecipitation in HEK293 cells. If the ternary complex is necessary to stimulate

phosphorylation of Lats1 hydrophobic motif by Mst2, disrupting one of the binding interactions within the ternary complex will inhibit the stimulation of phosphorylation of Lats1 hydrophobic motif by Mst2 caused by Mob1 co-expression.

Ni et al. isolated the ternary complex between Lats1 MBD, pMst2, and unphosphorylated Mob1 *in vitro* using gel filtration chromatography (Ni et al., 2015). However, they did not address whether the phosphorylation state of Mob1 may affect formation of the ternary complex. As previously stated, the NTE when unphosphorylated occupies the Lats1 binding site (Ni et al., 2015; Kim et al., 2016). On the other hand, when the Mob1 NTE is phosphorylated, it occupies the phospho-peptide binding pocket and forms a β-sheet with the Mob1 core domain - phosphorylated Mob1 NTE competes with the phosphorylated Mst2 linker domain to bind the same sites in the Mob1 core domain (Ni et al., 2015). We plan to isolate the ternary complex *in vitro* and answer whether the phosphorylation state of Mob1 affects ternary complex formation using a series of pull-down experiments. I plan to purify both phosphorylated Mob1, unphosphorylated Mob1, pMst2, and Lats1 MBD for use in the pull-down assay. Thus far, I have purified Lats1 MBD and developed a robust protocol for the expression and purification of Lats1 MBD.

Co-immunoprecipitation to capture and analyze protein:protein complexes

Introduction

Protein-protein interactions play a crucial role in many signaling pathways. In the Hippo tumor suppressor pathway, complex formation between Lats1 and Mob1 increases Lats1 kinase activity (Hergovich et al., 2006). Co-immunoprecipitation assays are used to isolate and identify protein complexes. The co-immunoprecipitation assay is a useful biochemical tool to map the binding interface of protein-protein interactions.

In co-immunoprecipitation, the protein of interest is isolated from cell lysate as a result of the protein being recognized by a specific antibody, and the antibody isolated by interactions with Protein G resin. Antibodies that recognize an epitope on the protein of interest are not always readily available, so often the protein of interest is expressed as an epitope-tagged fusion using tags such as Myc, HA, and FLAG tag that are recognized by commercially available antibodies. Following expression, lysate of cells expressing the epitope-tagged protein is mixed with the appropriate antibody. The antibody will bind the epitope-tagged protein ("bait") and when the protein:antibody complex is isolated any proteins that bind directly or indirectly to the protein of interest ("prey") will also be part of the antibody complex. The antibody-bound protein complex will be referred to as the "immunocomplex" (**Figure 4.1**). Immobilized Protein G resin is commonly used to precipitate the immunocomplex from solution. Protein G is a protein of the cell wall of group G streptococci that binds the Fc region of many subtypes of immunoglobulin G (IgG) (Kmiecik & Kolinski, 2008). By adding Protein G resin to the immunoprecipitation

reaction, Protein G will bind the antibody of the immunocomplex allowing for separation from cell lysate by centrifugation (**Figure 4.1**).

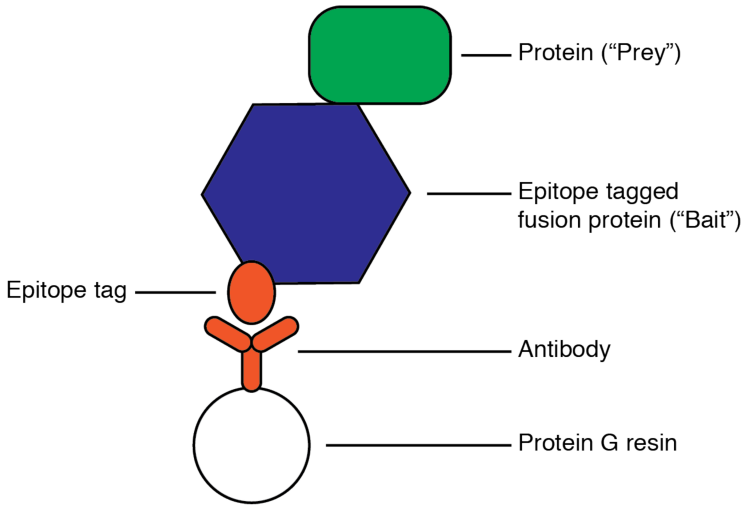

Figure 4.1: Schematic of immunoprecipitation of protein complexes
A schematic of the immunocomplex bound to Protein G resin. Protein G resin (white circle) binds to the antibody (orange) that recognizes the epitope tag of the bait protein (blue). If the bait binds to another protein (green), that protein is also isolated so long as the immunoprecipitation protocol does not disrupt complex formation.

The co-immunoprecipitation protocol must be adapted to account for biochemical differences among each protein complex. First, the stability of protein complexes differs in solution, and different buffer conditions under which protein complexes are captured may affect certain protein:protein interactions. Second, proteins may bind non-specifically to resin resulting in high background or false-positives. Third, proteins express differently in cells that may affect both capture of complex during immunoprecipitation and detection using Western blot analysis. Here, I describe the experiments conducted to develop a robust co-immunoprecipitation protocol for the Kavran Lab and explore different variables that need to be considered when designing a co-immunoprecipitation assay to isolate protein complexes. The Lats1 and Mob1 protein

complex was used as the model system for developing the co-immunoprecipitation assay because the protein complex had been purified and detected in vitro (Hergovich et al., 2006; Kim et al., 2016).

Materials and Methods

Transient transfection of HEK293 Cells

HEK293T cells were cultured in DMEM medium (Gibco) supplemented with 5% FBEssence (VWR) and 2mM Glutamine (Thermo Fischer) and grown at 37℃ and 5% CO_2. $0.9*10^6$ cells were seeded into 60mm dishes, and cells were transfected with pcDNA plasmids indicated in **Table 4.1** using polyethylenimine hydrochloride transfection reagent (PEI Max, Polysciences Inc.) at a ratio of 3µl of PEI Max to 1µg of DNA the following day. 48 hours after transfection, cell medium was aspirated, and cells were washed with 1mL ice-cold phosphate-buffered saline (PBS). PBS was aspirated, and cells were incubated with ice-cold immunoprecipitation buffer (IP buffer) (20mM Tris pH 8.0, 150mM NaCl, 1% Nonidet P-40 (NP-40), and 10% glycerol) supplemented with 50mM NaF, 1mM Na_3VO_4, 0.5mM PMSF, and Pierce Universal Nuclease (Thermo Scientific, 1:10,000) while rocking for 30 minutes at 4℃. Cell lysates were clarified by centrifugation at 23,000rpm for 10 minutes at 4℃. The total protein concentration in the lysate of each sample was quantified using the Pierce BCA protein assay kit (Thermo Scientific).

Table 4.1: DNA Plasmids used in transient transfection of HEK293T

Name	Epitope Tag	Protein	DNA Vector	Kavran Lab Code
Myc-Lats	Myc (EQKLISEEDL)	Lats1	pcDNA3.1 / 3x Myc-C	97
HA-Mob	HA (YPYDVPDYA)	Mob1	pcDNA3-HA	96

Immunoprecipitation and protein detection

0.5mg of total protein was loaded on to 20µL column volume (CV) of Protein G-Sepharose resin (GE Healthcare) with 1µg of α-HA antibody (Roche) for each co-

immunoprecipitation reaction. The reaction was conducted for 3 hours at 4℃. Resin was isolated by centrifugation at 1000g for 3 minutes, and supernatant was aspirated. Protein G resin was washed in batch 6 times with 1mL ice-cold IP buffer supplemented with 50mM NaF, 1mM Na3VO4, and 0.5mM PMSF. Proteins were eluted from Protein G resin by boiling for 5 minutes in 50µl 2.5X sodium dodecyl sulfate (SDS) gel agent. Samples were analyzed by Western blot.

Western blot analysis

In order to detect HA-Mob1 and Myc-Lats1, samples were resolved on 10 or 15% sodium dodecyl sulfate-polyacrylamide gel electrophoresis (SDS-PAGE) and transferred to nitrocellulose membranes (0.45µm) using the Trans-Blot Turbo Transfer System (Bio-Rad). Membranes were blocked in 5% skimmed milk powder in Tris-buffered saline (TBS: 20mM Tris pH 7.6 and 150mM NaCl) for 30 minutes at room temperature. Membranes were probed with either α-HA or α-Myc antibodies overnight at 4℃ (**Table 4.2**). Membranes were washed three times with TBS-T (20mM Tris pH 7.6, 150mM NaCl, 0.1% Tween 20) for 5 minutes. Then, membranes were incubated with fluorophore-conjugated secondary antibodies for 1 hour at room temperature (**Table 4.2**). The membranes were washed three times with TBS-T for 5 minutes. Blots were scanned on an Odyssey Infrared Imaging System (LI-COR) and analyzed using ImageStudio software (LI-COR).

Table 4.2: Antibodies used in Western blot analysis

Antibody	Host	Source	Reference	Dilution	Dilution Buffer	Repeated Use of Antibody?
c-Myc (9E10)	Mouse	Santa Cruz	sc-40	1:500	5% BSA in 1X TBS-T	No
HA	Rat	Roche	11867423001	1:1000	5% BSA in 1X TBS-T	1X
IRDye 680CW anti-Rat	Goat	LICOR	925-32219	1:10,000	5% Milk in 1X TBS-T	1X
IRDye 800CW anti-Mouse	Goat	LICOR	925-32210	1:10,000	5% Milk in 1X TBS-T	1X

Results

Selection of lysis buffer to maintain binding interaction

We tested different lysis buffers to determine how the binding interactions between Lats1 and Mob1 could be best preserved and Lats1 and Mob1 isolated as a protein:protein complex using co-immunoprecipitation. Initially, cells were lysed using RIPA buffer (25mM Tris pH 7.6, 150mM NaCl, 1% NP-40, 1% sodium deoxycholate, and 0.1% SDS) supplemented with 1mM Na_3VO_4 and 1mM PMSF. Under these conditions, Myc-Lats1 did not co-immunoprecipitate with HA-Mob1 (**Figure 4.2**). The detergents in RIPA buffer may have destabilized complex formation as ionic detergents can disrupt non-covalent bonds and alter the conformation of proteins. Instead, we screened a gentler version of the lysis buffer. IP buffer (20mM Tris pH 8.0, 150mM NaCl, 1% Nonidet P-40 (NP-40), and 10% glycerol) was substituted for RIPA to lyse the cells. IP buffer contains NP-40, a nonionic detergent that does not alter the conformation of proteins and glycerol that can help stabilize protein complexes *in vitro* (Johnson, 2013). When IP buffer was used to lyse the cells, Myc-Lats1 co-immunoprecipitated with HA-Mob1 (**Figure 4.2**). For all subsequent experiments, IP buffer was used to lyse cells.

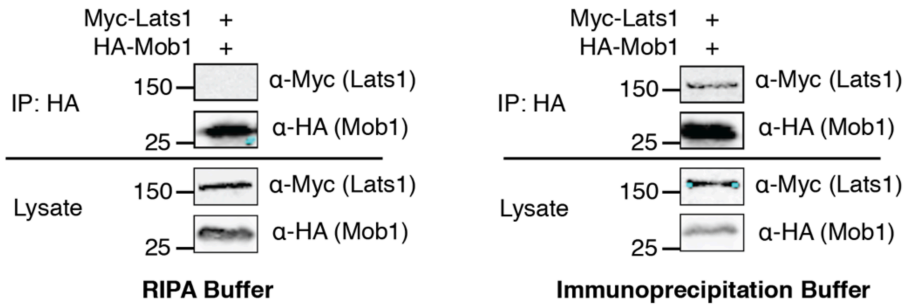

Figure 4.2: Lysis buffer may disrupt protein:protein interactions
HEK293 cells co-transfected with Myc-Lats1 and HA-Mob1. RIPA buffer (left) or IP buffer (right) was used to lyse cells to determine which lysis buffer best preserves protein:protein interactions. HA (Mob1) was immunoprecipitated, and immunoblots following immunoprecipitation are shown to analyze capture of Myc-Lats1 and HA-Mob1. Cell lysates were probed for protein expression using Western blot analysis with antibodies specific to epitope-tags (Myc and HA).

Establishing positive and negative controls

We established controls to demonstrate that detection of protein:protein complex following co-immunoprecipitation was not a result of non-specific interactions. First, we needed to prove that detection of the protein complex is not the result of false, non-specific interactions with Protein G resin. Lysate of HEK293 cells transfected with HA-Mob1 and Myc-Lats1 was incubated with Protein G resin. HA-Mob1 bound to Protein G resin while Myc-Lats1 did not (**Figure 4.3A**). We screened different wash conditions to minimize non-specific interactions with Protein G resin and HA-Mob1. When Protein G resin was washed three times with 500μL IP buffer (Wash Condition #1), HA-Mob1 still bound to resin (**Figure 4.3A**). When resin was washed six times with 1mL IP buffer (Wash Condition #2), HA-Mob1 did not interact with Protein G resin (**Figure 4.3A**).

Next, we validated that the detection of the "prey" protein, Myc-Lats1, was not the result of false interaction with the antibody used for immunoprecipitation; rather, Myc-Lats1 detection is a result of specific protein:protein interaction between the "bait," HA-Mob1, and "prey," Myc-Lats1. Lysate of HEK293 cells transfected with Myc-Lats1

was incubated with Protein G resin and α-HA antibody, and Myc-Lats1 was not detected (**Figure 4.3B**).

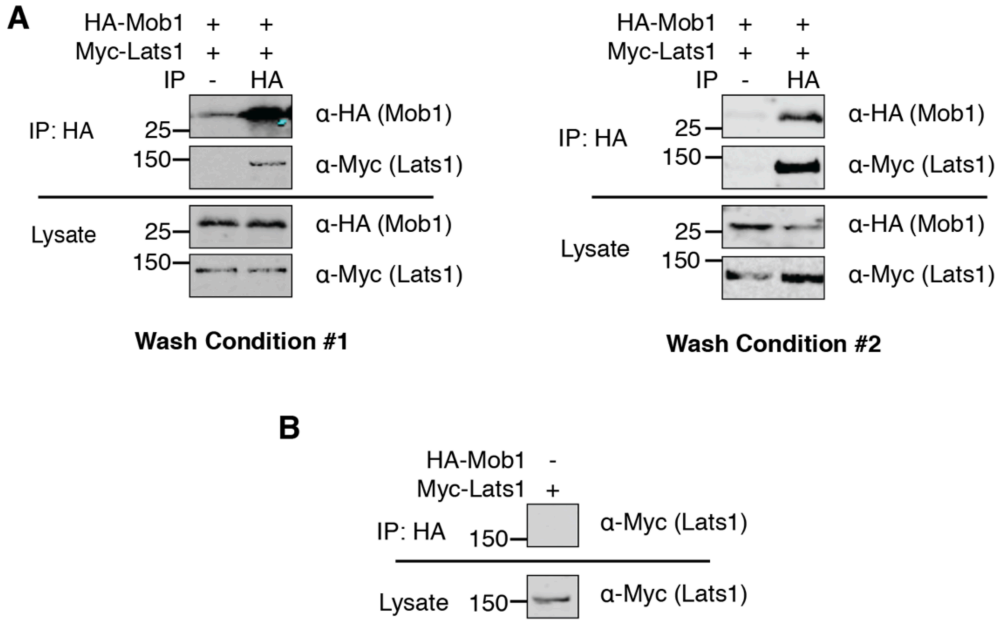

Figure 4.3: Minimizing non-specific interactions to establish a negative control
A. Myc-Lats1 and HA-Mob1 were co-transfected into HEK293 cells. Cell lysate was incubated with Protein G resin to determine whether expressed proteins interact with resin in the absence of antibody. Different wash conditions were used to minimize non-specific interaction between HA-Mob1 and Protein G resin. Wash Condition #1: Protein G resin was washed three times with 500μL IP buffer (left). Wash Condition #2: Protein G resin was washed six times with 1mL IP buffer (right). HA (Mob1) was immunoprecipitated to validate that the wash conditions did not interfere with capture of protein:protein complex. Immunoblots following immunoprecipitation are shown to analyze capture of Myc-Lats1 and HA-Mob1. A fraction of cell lysate was analyzed using Western blot analysis for protein expression using antibodies specific to the epitope tags (Myc and HA). **B.** Lysate of HEK293 cells transfected with Myc-Lats1 was incubated with Protein G resin and α-HA antibody to confirm that Myc-Lats1 does not interact with α-HA antibody. Immunoblots following immunoprecipitation are shown. A fraction of cell lysate was analyzed using Western blot analysis for protein expression using antibody specific to the epitope tag (Myc).

Improving efficiency of Lats1-Mob1 isolation

We wanted to determine what variables could be changed to increase capture and improve detection of the protein complex. For this model system, it was difficult to detect HA-Mob1 and Myc-Lats1 using co-immunoprecipitation (**Figure 4.4**). This result could arise from multiple factors including low abundance of Myc-Lats1 or weak binding interaction between the proteins.

First, the amount of total cell lysate that was loaded to Protein G resin was changed to see if increasing the abundance of Myc-Lats1 and HA-Mob1 could increase the likelihood of capture of protein:protein complex from cell lysate. Either 0.15mg or 0.5mg of total protein in cell lysate was loaded. Increasing the total amount of cell lysate did not increase capture of Myc-Lats1 (**Figure 4.4**).

Next, we increased the amount of antibody incubated in the immunoprecipitation reaction to increase the amount of protein complex that could be isolated and the likelihood of capture of protein:protein complex. Cell lysate was incubated with either 0.2μg or 2μg of α-HA antibody. Unfortunately, increasing the amount of α-HA antibody used for immunoprecipitation did not increase capture of Myc-Lats1 (**Figure 4.4**). On the other hand, when both variables were increased - 2μg of α-HA antibody and 0.5mg of total protein - the amount of Myc-Lats1 detected to co-immunoprecipitate increased (**Figure 4.4**).

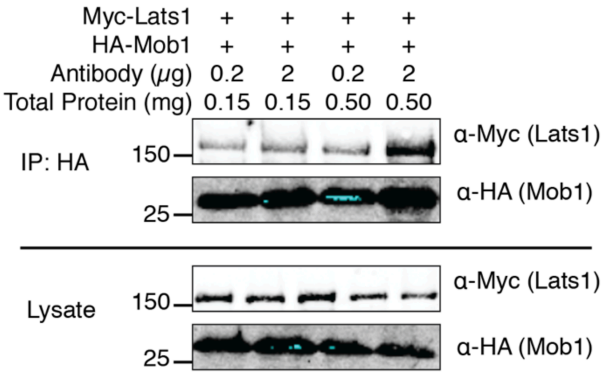

Figure 4.4: Increasing the detection of Lats1 and Mob1 protein complex
HEK293 cells were transiently transfected with HA-Mob1 and Myc-Lats1. Two variables were changed to determine how to best increase capture of protein:protein complex of Myc-Lats1 and HA-Mob1 using immunoprecipitation from lysate of HEK293 cells. HA-Mob1 was immunoprecipitated from 0.15mg or 0.5mg of total protein in cell lysate using 0.2µg or 2µg of α-HA antibody. Cell lysate and immunoprecipitation were analyzed by Western blot analysis using indicated antibodies to detect protein expression and capture of protein:protein complex.

Discussion

Co-immunoprecipitation protocols must be optimized for different protein:protein complexes as the strength and nature of each varies. The experiments described here establish a co-immunoprecipitation protocol for use in the Kavran Lab. Three variables were analyzed to optimize the co-immunoprecipitation protocol: selection of lysis buffer, wash condition to remove non-specific binding interactions, and capture of protein complex.

It is critical to select a lysis buffer that will not destabilize protein complexes. In these experiments, use of IP buffer results in capture of Myc-Lats1 and HA-Mob1 as a protein complex while use of RIPA buffer does not (**Figure 4.2**). Use of IP buffer better preserves the native conformation of proteins and binding interactions within protein:protein complexes due to the use of nonionic detergents.

Proper negative controls must be included for each co-immunoprecipitation experiment to demonstrate that the prey protein does not interact non-specifically with either the antibody or resin used in immunoprecipitation. When met, this control ensures that if any co-immunoprecipitation of the prey protein is detected in later experiments, it is a consequence of interaction between the bait and prey. Here, wash conditions affect non-specific interactions between HA-Mob1 and Protein G resin. Increasing the volume – 500µl to 1mL of buffer – and the number of washes – 3 washes to 6 washes – is sufficient to eliminate non-specific interaction between Protein G resin and HA-Mob1 (**Figure 4.3A**). However, care must be taken to ensure that the stringency of the wash conditions not disrupt protein:protein interactions.

Although two proteins may form a complex, the abundance of the protein of interest affects detection following co-immunoprecipitation. The likelihood of capturing Myc-Lats1 and HA-Mob1 as a protein complex increased by increasing the amount of antibody used for immunoprecipitation and the amount of total cell lysate present in solution (**Figure 4.4**). I find it optimal to use 0.5mg of total protein cell lysate and 1µg of antibody for capture of Lats1 and Mob1 as a protein:protein complex. For other protein:protein complexes, the abundance of each protein may vary, and these variables may have to be optimized on a case-by-case basis.

Purification of Protein G' for use in co-immunoprecipitation

Introduction

Co-immunoprecipitation assays are a standard technique used to isolate protein complexes from cell lysate and are commonly used in the Kavran Lab. In this assay, an antibody binds the protein of interest, and the complex is isolated by immobilized Protein G' resin. We wanted to develop a protocol to express and purify our own immobilized Protein G' resin as Protein G' resin is expensive (**Table 5.1**).

Protein G is used for immunoprecipitation (IP) assays because of its specificity and affinity to immunoglobulin G (IgG). In nature, Protein G is a component of the cell wall of group G streptococci. Protein G has been applied for use in biochemical studies because it binds to the Fc region of immunoglobulin as well as many subtypes of IgG in the C-terminal region of Protein G (Eliasson et al., 1991). However, Protein G cannot bind IgM, IgD, or IgA (Bjorck & Kronvall, 1984). Commercially available Protein G resins use a modified variant (Protein G') in which the N-terminal region is truncated to prevent binding to human serum albumin. Thus, the use of recombinant Protein G' in co-immunoprecipitation ensures binding to only IgG.

Here, we aim to develop a protocol to make an immobilized Protein G' resin for use in IP assays. We first determined suitable expression and purification conditions for Protein G'. We asked whether our Protein G' coupled to resin captures protein:protein interactions with the same efficiency as commercial resin using co-immunoprecipitation. The Mst2/Mob1 protein complex was used as a positive control (Kulaberoglu et al., 2017).

Table 5.1: Price of Protein G' resin

Product Name	Source	Catalog Number	Price ($) / (1mL Column Volume)
Protein G Agarose	Sigma	11243233001	129.2
Protein G Resin	GE Healthcare	17061801	105.8
Pierce Protein G Agarose	Thermo Fischer Scientific	20399	83.6

Table 5.2: Protein G' sequence and vectors used for protein expression

Recombinant Protein G' Amino Acid Sequence	Vector	Affinity Tag
LPKTDTYKLILNGKTLKGETTTEAVDAATAEKVFKQ YANDNGVDGEWTYDDAT KTFTVTEKPEVIDASELTPAVTTYKLVINGKTLKGET TTEAVDAATAEKVFK	pSATL	H6SUMO
QYANDNGVDGEWTYDDATKTFTVTEKPEVIDASEL TPAVTTYKLVINGKTL KGETTTKAVDAETAEKAFKQYANDNGVDGVWTYD DATKTFTVTE	p2AT	-

Materials and Methods

Cloning and expression of Protein G'

A codon optimized gene encoding *streptococcal Protein G'* for expression in E.coli was ordered from GeneArt (**Table 5.2**). The gene was cloned into either a pSAT-L vector downstream from a hexahistidine and SUMO tag (H_6SUMO) or p2AT vector without a tag. Both H_6SUMO-Protein G' and untagged Protein G' were expressed in T7 Express cells (New England BioLabs), and growth and induction methods were the same for both expressions. Transformed T7 Express cells grew at 37°C in LB media. Protein expression was induced at 0.5 OD_{600} with 0.5mM IPTG and harvested after 3 hours.

Purification of H_6SUMO-Protein G' (pSAT-L vector)

Cells grown in 1L of LB media were lysed in 50mL of lysis buffer (50mM Tris pH 8.0, 400mM NaCl, and 5% glycerol) supplemented with protease inhibitor cocktail (Sigma-Aldrich) using the micro-fluidizer. Cell lysate was clarified by centrifugation at 23,000rpm for 30 minutes at 4°C. Supernatant was incubated with 5mL column volume (CV) of Profinity-IMAC resin (Bio-Rad) for 1 hour, rotating, at 4°C. Resin was collected by centrifugation at 1000g for 5 minutes at 4°C, and supernatant aspirated. Resin was washed in batch twice with 5CV of lysis buffer and three times with 5CV of lysis buffer supplemented with 10mM Imidazole. Protein G' was eluted with 50mM Tris pH 8.0, 400mM NaCl, 5% glycerol, and 125mM Imidazole. Protein was dialyzed into 20mM Tris pH 7.0, 100mM NaCl, 5% glycerol, in the presence of 0.17μM SUMO-specific protease (SENP) for cleavage of the H_6SUMO tag at 4°C overnight (Malakhov et al., 2004). Following dialysis, protein was clarified by centrifugation at 23,000rpm for 30 minutes at

4°C. The supernatant was diluted with 10mM Tris pH 8.0 to lower the concentration of NaCl to 50mM and loaded onto a 5mL CV Hi Trap Q HP column (GE Healthcare). Protein was eluted with an increasing concentration gradient of NaCl. Fractions containing Protein G' were pooled and loaded on a HiLoad 16/600 Superdex 75 size exclusion column (GE Healthcare) equilibrated in 10mM HEPES pH 7.5 and 200mM NaCl. Fractions containing Protein G' were concentrated to 25mg/mL and flash frozen in liquid nitrogen.

Purification of untagged Protein G' (p2AT vector)

Cells grown in 4L of LB Media were lysed in 100mL of lysis buffer supplemented with protease inhibitor cocktail (Sigma-Aldrich) using the micro-fluidizer. Lysate was clarified by centrifugation at 23,000rpm for 30 minutes at 4°C. Supernatant was diluted with sufficient volume of 10mM Tris pH 8.0 to reduce the final concentration of NaCl to 50mM and loaded onto a 5mL Hi Trap Q HP anion exchange column. Protein G' was eluted using an increasing concentration gradient of NaCl. Fractions containing Protein G' were pooled and loaded on a HiLoad 26/600 Superdex 75 size exclusion column (GE Healthcare) equilibrated in 10mM HEPES pH 7.5 and 200mM NaCl. Fractions containing Protein G' were concentrated to 6.9mg/mL and flash frozen in liquid nitrogen.

Coupling Protein G' to resin

Profinity Epoxide Resin (Bio-Rad) coupling reaction

Resin was swelled in 10CV of water rotating for 30 minutes at room temperature (1g of resin swells to 8mL CV). Resin was collected by centrifugation at 1000g for 5 minutes at

4°C, and supernatant aspirated. Purified Protein G' was diluted using 100mM $NaHCO_3$ pH 11.3 to a final volume of 2CV of swelled resin and added to resin (2mg Protein G' per 1mL CV of swelled resin). Resin and protein were incubated for 10 minutes at room temperature while gently rocking. 800mg of $AmSO_4$ per 1mL CV of swelled resin was added to the coupling reaction, which was then left overnight at room temperature with gentle rocking. The concentration of protein present before and after the coupling reaction was measured to monitor completion of the reaction. When the reaction was complete, resin was collected by centrifugation at 1000g for 5 minutes at 4°C, and supernatant was aspirated. 10CV of 1M ethanolamine pH 8.0 was added to the resin and the slurry incubated for 4 hours at room temperature with gentle rocking. Resin was collected by centrifugation at 1000g for 5 minutes at 4°C, and supernatant was aspirated. Resin was washed three times in batch with 5CV of 20mM Tris pH 8.0 and 200mM NaCl. Resin was stored in 20mM Tris pH 8.0, 200mM NaCl, and 0.1% NaN_3 as a 10% slurry at 4°C.

CnBr-Activated Sepharose 4 Fast Flow (GE Healthcare) coupling reaction

Resin was swelled in 10CV of 1mM HCl for 30 minutes at 4°C while gently rocking (1g of resin swells to 5mL CV). Resin was collected by centrifugation at 1000g for 5 minutes at 4°C, and supernatant aspirated. Resin was washed in batch three times with 5CV of 1mM HCl and once with 5CV of 10mM HEPES pH 7.5 and 200mM NaCl. Protein was diluted using 10mM HEPES pH 7.5 and 200mM NaCl to a final volume of 2CV of swelled resin and added to resin (2mg of Protein G' per 1mL CV of resin). The coupling reaction was left at 4°C overnight while gently rocking. The concentration of protein in

solution prior to and after the coupling reaction was measured to monitor the progress of the reaction. Resin was collected by centrifugation at 1000g for 5 minutes at 4°C, and supernatant aspirated. Resin was incubated with 5CV of 10mM HEPES pH 7.5 and 200mM NaCl for 30 minutes at room temperature. Resin was collected by centrifugation at 1000g for 5 minutes at 4°C, and supernatant was aspirated. Resin was incubated in 10CV of 100mM Tris pH 8.0 for 3 hours at room temperature with gentle rocking to quench the reaction. Resin was collected by centrifugation at 1000g for 5 minutes at 4°C, and supernatant was aspirated. Resin was washed in batch with 10CV of 100mM Tris pH 8.0 and 500mM NaCl. Protein G'-coupled resin was stored in 10% EtOH as a 10% slurry at 4°C.

Transient transfection of HEK293 Cells

The methods detailed in the co-immunoprecipitation chapter were used in this experiment. The pcDNA plasmids transfected into HEK293T cells are indicated in **Table 5.3**

Table 5.3: DNA Plasmids used in transient transfection of HEK293

Name	Peptide Tag	Protein	DNA Vector	Kavran Lab Code	DNA Transfected (ug)/Well
FLAG-Mob1	FLAG (DYKDDDDK)	Mob1	pcDNA3-FLAG	JA	1
HA-Mst2	HA (YPYDVPDYA)	Mst2	pcDNA3-HA	94	1

Co-Immunoprecipitation

The methods detailed in the co-immunoprecipitation chapter were used in this experiment. α-FLAG (Sigma) and α-HA (Roche) antibodies were used.

Western blot analysis

In order to detect FLAG-Mob1 and HA-Mst2, samples were resolved using 15% sodium dodecyl sulfate-polyacrylamide gel electrophoresis (SDS-PAGE) and transferred to nitrocellulose membranes (0.45µm) using the Trans-Blot Turbo Transfer System (Bio-Rad). Membranes were blocked in 5% skimmed milk powder dissolved in Tris-buffered saline (20mM Tris pH 7.6 and 150mM NaCl) for 30 minutes at room temperature. Membranes were probed with α-FLAG and α-HA antibodies overnight at 4℃ (**Table 5.4**). Membranes were washed three times with TBS-T (20mM Tris pH 7.6, 150mM NaCl, and 0.1% Tween 20) for 5 minutes. Then, membranes were incubated with fluorophore-conjugated secondary antibodies for 1 hour at room temperature (**Table 5.4**). The membranes were washed three times with TBS-T for 5 minutes. Blots were scanned on an Odyssey Infrared Imaging System (LI-COR) and analyzed using ImageStudio software (LI-COR).

Table 5.4: Antibodies used in Western blot analysis

Antibody	Host	Source	Reference	Dilution	Dilution Buffer	Repeated Use of Antibody?
FLAG	Mouse	Sigma	F1840	1:1000	5% BSA in 1X TBS-T	1X
HA	Rat	Roche	11867423001	1:1000	5% BSA in 1X TBS-T	1X
IRDye 680CW anti-Rat	Goat	LICOR	925-32219	1:10,000	5% Milk in 1X TBS-T	1X
IRDye 800CW anti-Mouse	Goat	LICOR	925-32210	1:10,000	5% Milk in 1X TBS-T	1X

Results

Small-scale expression and solubility tests of Protein G'

Small-scale expression tests were performed to determine the best conditions for both H_6SUMO-Protein G' and untagged Protein G' expression and solubility. Proteins were expressed in a BL21 strain of E.coli and grown in LB media. Protein expression was induced with IPTG when the cells entered mid-log, and cells grew at either 37°C for 3 hours or 20°C overnight following induction. Samples of cell lysate taken before induction and at the time of harvest were resolved using Coomassie stained SDS-Page to determine expression of both H_6SUMO-Protein G' and untagged Protein G' (**Figure 5.1**). There was no difference in expression for either H_6SUMO-Protein G' or untagged Protein G' under both growth conditions. Samples of cell lysate and supernatant following clarification of cell lysate were analyzed using Coomassie stained SDS Page to determine both H_6SUMO-Protein G' and untagged Protein G' solubility. Solubility of H_6SUMO-Protein G' appeared to be slightly improved when cells were grown at 37°C for 3 hours following induction (**Figure 5.1A**). Solubility of untagged Protein G' did not differ (**Figure 5.1B**). The optimal condition for expression and solubility of both H_6SUMO-Protein G' and untagged Protein G' is growth at 37°C for 3 hours following induction at 0.5 OD_{600}.

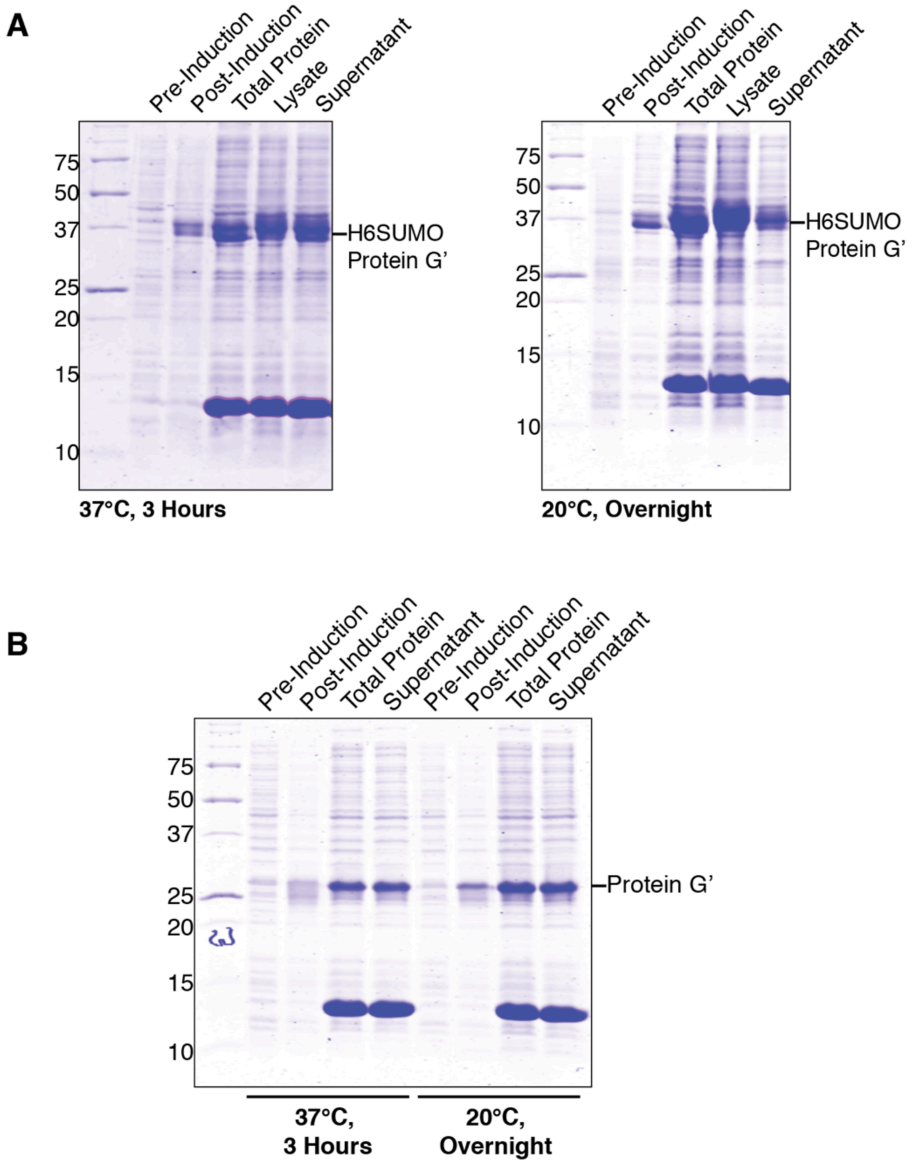

Figure 5.1: Small-scale Protein G' expression and solubility tests
A. Analysis of H_6SUMO-Protein G' expression and solubility using Coomassie stained SDS Page. (Left) Tests conducted when transformed T7 Express cells were grown at 37°C for 3 hours following induction. (Right) Tests conducted when transformed T7 Express cells were grown at 20°C overnight following induction. **B.** Analysis of H_6SUMO-Protein G' expression and solubility using Coomassie stained SDS Page. The first four lanes are of tests conducted when T7 Express cells were grown at 37°C for 3 hours following induction and the last four lanes when T7 Express cells were grown at 20°C overnight following induction.

Purification of H_6SUMO-Protein G'

We tried to purify both H_6SUMO-Protein G' and untagged Protein G' to determine the easiest purification scheme of Protein G' with high yield and purity. Different methods were used to purify H_6SUMO-Protein G' and untagged Protein G'. We first isolated H_6SUMO-Protein G' using IMAC (**Figure 5.2A**). H_6SUMO-Protein G' was present in the flow-through that indicated two possible scenarios: there was insufficient resin to bind all of H_6SUMO-Protein G' present in cell lysate or H_6SUMO-Protein G' aggregated resulting in an inability of the affinity tag to bind the Profinity-IMAC resin. The flow-through was loaded onto a small-scale affinity purification to determine if the unbound H_6SUMO-Protein G' was capable of binding nickel resin (**Figure 5.2B**). On the second round of affinity purification, H_6SUMO-Protein G' bound and eluted from resin indicating that there was insufficient resin in the first affinity purification step to capture all H_6SUMO-Protein G' present in cell lysate. We thus determined H_6SUMO-Protein G' binds Profinity-IMAC resin and elutes from resin while maintaining solubility.

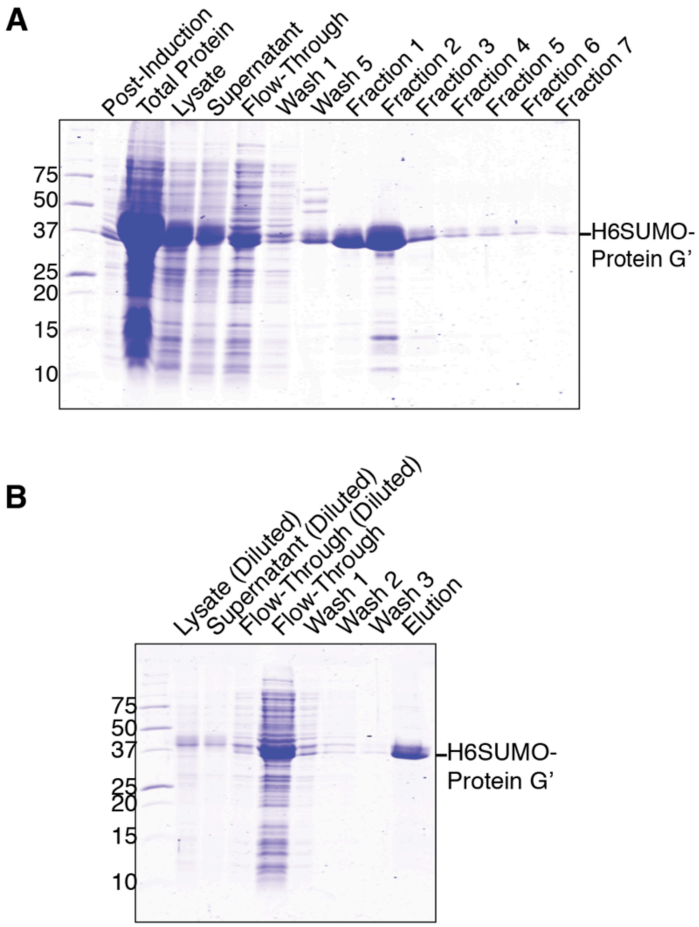

Figure 5.2: IMAC Purification of H_6SUMO-Protein G'
A. Expression and IMAC Purification of H_6SUMO-Protein G' is shown using Coomassie stained SDS-Page. Fractions containing H_6SUMO-Protein G' were pooled for further purification. **B.** Flow-through of initial IMAC purification was loaded onto Profinity-IMAC resin for a secondary small-scale IMAC purification to determine why H_6SUMO-Protein G' was present in the flow-through. Lysate, supernatant, and flow-through from initial IMAC purification were diluted tenfold before loading onto Coomassie stained SDS-Page. Flow-through, wash fractions, and elution of second IMAC purification are resolved on Coomassie stained SDS-Page.

The next step in purification is cleavage of the affinity tag from Protein G'. IMAC elution fractions containing H_6SUMO-Protein G' were pooled and incubated with SENP during dialysis. Efficient cleavage of the affinity tag is demonstrated in **Figure 5.3**.

We used anion exchange chromatography followed by gel filtration chromatography to separate the affinity tag from untagged Protein G'. The peaks containing either the tag or Protein G' partially overlapped; three of the four fractions of the Protein G' peak did not contain H_6SUMO, but one of the fractions had some tag present (**Figure 5.3**). All four fractions were pooled and loaded onto gel filtration chromatography, which separated the affinity tag from Protein G' (**Figure 5.4**). The final yield of Protein G' expressed as H_6SUMO-Protein G' was 1.5mg of Protein G' per 1L of cells.

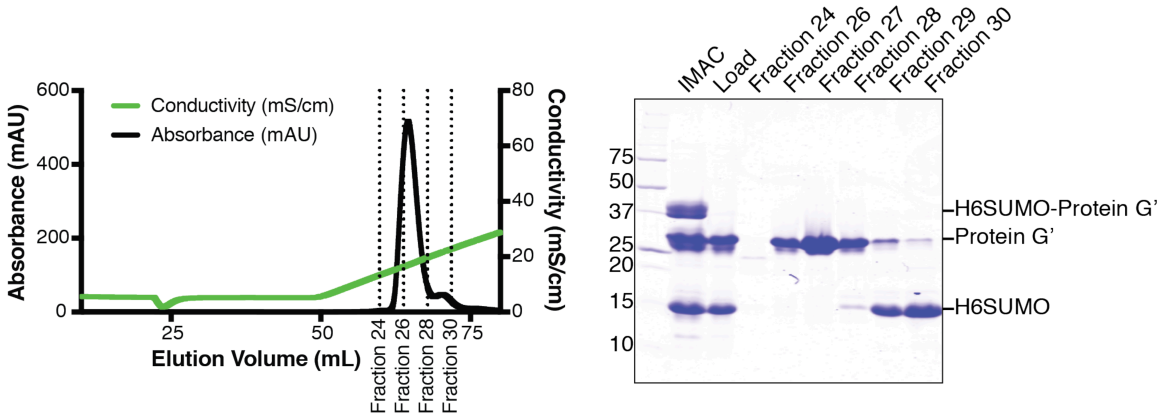

Figure 5.3: Affinity tag cleavage of H_6SUMO-Protein G' and anion exchange chromatography

SENP was added to cleave the affinity tag from H_6SUMO-Protein G' during dialysis. Tag cleavage of H_6SUMO-Protein G' is demonstrated by comparing IMAC and load lanes in Coomassie stained SDS-Page gel. Following dialysis and affinity tag cleavage, anion exchange chromatography was completed. There was near separation of H_6SUMO and Protein G'. However, there was slight contamination in Fractions 28 - 29. Fractions 26-28 containing Protein G' were pooled for further purification.

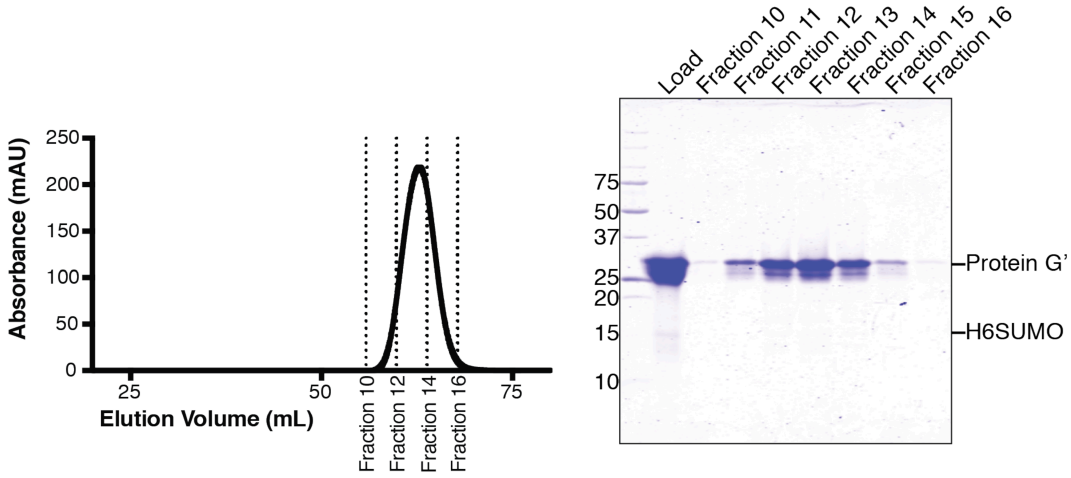

Figure 5.4: Separation of Protein G' from H_6SUMO affinity tag using gel filtration chromatography

Chromatogram of gel filtration and accompanying Coomassie stained SDS-Page are displayed. Fractions 11 - 15 containing Protein G' were pooled and concentrated to 25.05mg/mL. H_6SUMO was not present in fractions pooled. The final yield was 1.5mg Protein G'/L of cell growth.

Purification of Protein G' expressed as untagged protein

We tried to purify an untagged variant of Protein G' to avoid the challenges associated with tag cleavage and separation. However, we were concerned as to how efficiently Protein G' could be isolated. Untagged Protein G' was expressed as described above and clarified cell lysate was loaded directly onto the anion exchange column (**Figure 5.5**). Protein G' eluted at a lower conductivity than Protein G' expressed as H_6SUMO-Protein G' and was only 55% pure. Capture of Protein G' was inefficient, as evidenced by presence of Protein G' in the flow-through and wash fractions indicating that the column volume was insufficient to capture all of the Protein G' from cell lysate (**Figure 5.5**). The fractions containing Protein G' were pooled and loaded onto a gel filtration column. Peak fractions were collected and concentrated (**Figure 5.6**). The final yield of Protein G' was 6.5mg of Protein G' per 1L of cells but was only 86% pure.

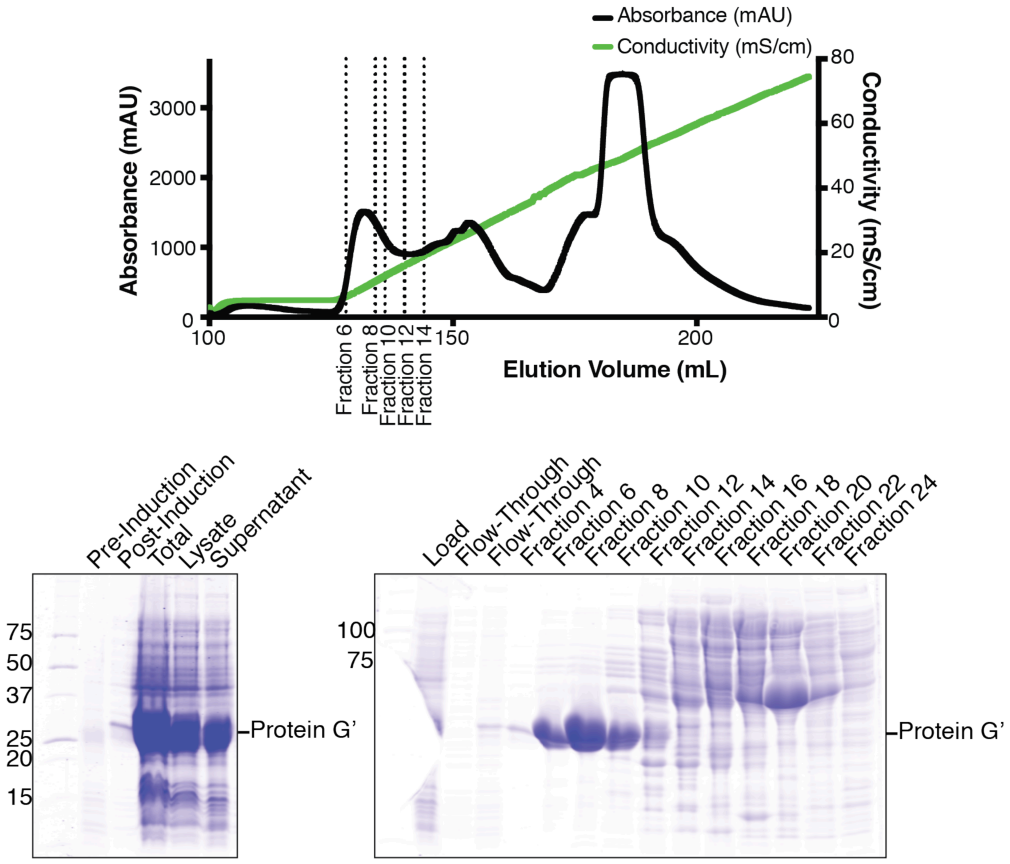

Figure 5.5: Purification of Protein G' expressed as untagged Protein G' using anion exchange chromatography

Expression and solubility of untagged Protein G' following lysis are displayed on the left Coomassie stained SDS-Page Gel. Chromatogram of purification of untagged Protein G' using anion exchange is shown with corresponding Coomassie stained SDS-Page Gel (right). Fractions 6 - 9 containing Protein G' were pooled for further purification.

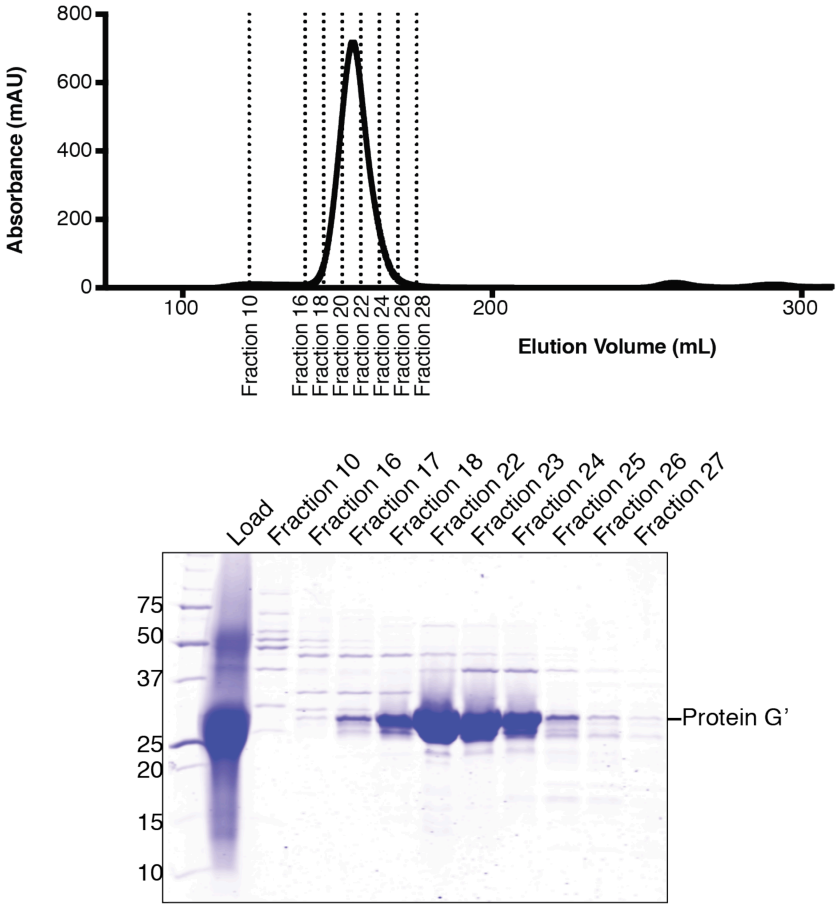

Figure 5.6: Purification of untagged Protein G' using gel filtration chromatography
Chromatogram of gel filtration and the accompanying Coomassie stained SDS-Page Gel are displayed. Fractions 17 - 25 containing Protein G' were pooled and concentrated to 6.895mg/mL. The final yield was 6.5mg of Protein G'/L of cell growth.

Testing the efficiency of purified Protein G' coupled to resin in co-immunoprecipitation

Next, we wanted to determine whether our recombinant Protein G' when coupled to resin had the same efficiency as commercial Protein G' resin in co-immunoprecipitation. Purified Protein G' was coupled to two resins - Profinity Epoxide resin (Bio-Rad) and CnBr-activated Sepharose 4 Fast Flow (GE Healthcare) - to analyze whether different coupling chemistry and resins could affect the use of recombinant Protein G' in co-immunoprecipitation (**Figure 5.7**). Then, the efficiency of the resin was measured by two criteria – the coupled resin needed to have the same non-specific binding pattern and the same ability to immunoprecipitate a protein:protein complex as commercial Protein G' resin.

First, Protein G' resin was incubated with lysate of HEK293 cells transiently transfected with HA-Mst2 and FLAG-Mob1 in the absence of antibody to examine whether the resin would interact nonspecifically with either protein of interest (**Figure 5.7**). Protein G' coupled to CnBr-Activated Sepharose 4 Fast Flow resin bound HA-Mob1 non-specifically. Nonspecific interactions between Protein G' coupled to Profinity Epoxide resin with FLAG-Mob1 and HA-Mst2 was comparable to that of commercial Protein G' resin.

Next, Mst2:Mob1 protein:protein complex was immunoprecipitated from lysate of HEK293 cells transiently transfected with HA-Mst2 and FLAG-Mob1 to determine whether recombinant Protein G' coupled to resin captures protein:protein complex similar to commercial Protein G' resin (**Figure 5.7**). Purified Protein G' coupled to CnBr-Activated Sepharose 4 Fast Flow resin captured less of the protein complex of

interest as compared to Protein G' coupled to Profinity Epoxide resin or commercially available resin. Protein G' coupled to Profinity Epoxide resin demonstrated similar capture of HA-Mst2 and FLAG-Mob1.

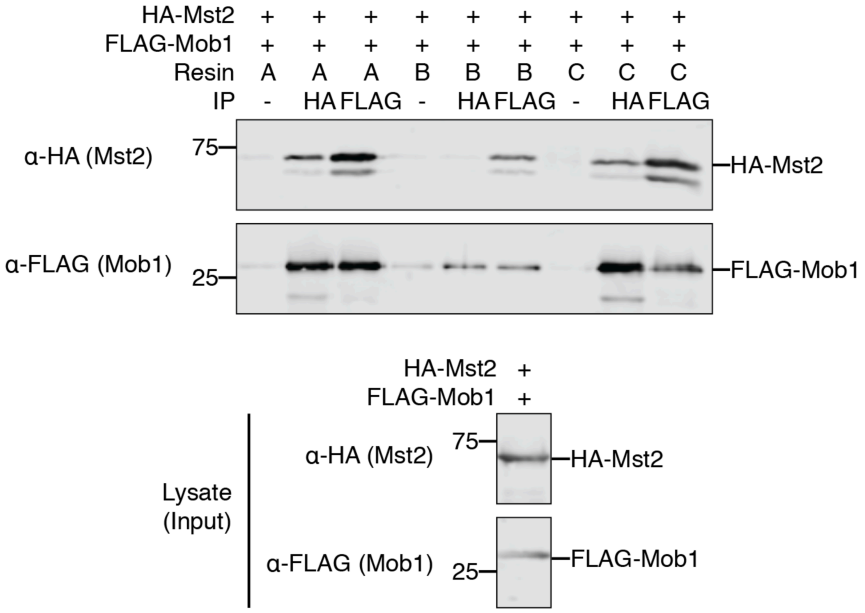

CnBr-activated Sepharose 4 Fast Flow (GE Healthcare) - Resin B		
	Absorbance (280)	Concentration (uM)
Pre-Coupling	1.27	42.59
Post-Coupling	0.55	18.39

Profinity Epoxide Resin (Bio-Rad) - Resin C		
	Absorbance (280)	Concentration (uM)
Pre-Coupling	1.27	42.59
Post-Coupling	0.53	17.72

Figure 5.7: Testing the efficiency of Protein G' resin using co-immunoprecipitation
HEK293 cells were transiently transfected with HA-Mst2 and FLAG-Mob1. Normalized cell lysate was loaded to three different Protein G' resins. Resin A was Protein G Sepharose 4 Fast Flow produced commercially. Resin B was purified Protein G' coupled to CnBr-Activated Sepharose 4 Fast Flow. Resin C was purified Protein G' coupled to Profinity Epoxide resin. Protein G' resin was incubated with cell lysate and either α-HA antibody, α-FLAG antibody, or no antibody. Following immunoprecipitation, HA-Mst2 and FLAG-Mob1 were detected using Western blot analysis. Cell lysate was also probed with HA and FLAG antibodies to demonstrate expression of HA-Mst2 and FLAG-Mob1. The concentration of Protein G' before and after the coupling reaction is reported in the two tables.

Discussion

Protein G has been applied for use in immunoprecipitation as it can bind the Fc region of both monoclonal and polyclonal IgG (Eliasson et al., 1991). In the experiments described here, we determined protocols for the purification of two variants of Protein G' – one for H_6SUMO-Protein G' and the other for untagged Protein G'. We also validated that purified recombinant Protein G' can be coupled to resin and used in immunoprecipitation as efficiently as commercial Protein G' resin.

Purification of H_6SUMO-Protein G' requires additional steps in comparison to the purification of untagged Protein G': cleavage and removal of the affinity tag. Our initial purification of tagged Protein G' suffered from poor capture resulting from insufficient IMAC resin. Thus, the yields from this purification are not indicative of those expected from future purifications. I estimate that the yield could be improved 3X fold if the CV were increased to 15ml/L of cells to ensure full capture of the protein (**Figure 5.2**). Anion exchange and gel filtration chromatography result in complete separation of H_6SUMO and Protein G' (**Figure 5.3, 5.4**). Purification of untagged Protein G' also suffered from poor capture from the initial lysate, and future preps would require using 10mL CV of Hi Trap Q Column per 4L of cells. Overloading of the column also resulted in premature elution of Protein G' causing, possibly, co-elution with contaminating proteins (**Figure 5.5**).

We decided to purify untagged Protein G' to make our resin. First, the yield of Protein G' expressed as untagged protein was significantly higher than that of Protein G' expressed with the affinity tag. Second, for future purifications, we can increase the column volume during anion exchange chromatography to decrease contaminants present

by preventing premature elution of Protein G'. Last, the purification of Protein G' expressed as untagged protein is significantly less time-consuming than of Protein G' expressed with the affinity tag. Ultimately, we can resolve the initial concern of isolation of untagged Protein G' from cell lysate while maximizing yield and minimizing the difficulty of purification.

Purified Protein G' can be coupled to resin for use in co-immunoprecipitation. Here, we screened two different coupling chemistry and bead types (Profinity Epoxide and CnBr-Activated Sepharose 4 Fast Flow) and found Protein G' coupled to Profinity Epoxide resin performed similarly to commercial resin in side-by-side comparisons that evaluated both non-specific binding and capture efficiency (**Figure 5.7**). Thus, it is recommended that Protein G' be coupled to Profinity Epoxide resin for use in co-immunoprecipitation.

Conclusion

We conducted a series of experiments for co-immunoprecipitation protocol optimization. The variables tested – selection of lysis buffer, capture of protein complex, and preventing non-specific interactions – are a good starting point to reference for protocol optimization. Here, co-immunoprecipitation was used to study the binding interactions between protein:protein complexes. Furthermore, the tools and methods learned from the purification of Protein G' for use in co-immunoprecipitation were applied for the purification of Lats1 MBD and will be applied for purifying Mob1 and Mst2 for the analysis of ternary complex formation (Lats1-Mob1-Mst2) *in vitro*.

This study aims to elucidate the molecular mechanism for Lats1 kinase further. We focused on analyzing Lats1 kinase activation from two perspectives. First, we identified regions of the Lats1 N and C termini that are necessary for Lats1 function to define a minimal, functional unit of Lats1 kinase to express and purify *in vitro* for future biochemical and structural assays. We examined Lats1 kinase function using two criteria thus far: binding to Mob1, a co-activator, and kinase activity analyzed by downstream pathway function and substrate phosphorylation. Going forward, we plan to test whether the N-terminal truncated Lats1 variant 635 [GJ] can bind Mob1 using more sensitive detection methods following co-immunoprecipitation.

Due to time restraints, we were unable to examine the third criteria for Lats1 kinase activation: phosphorylation of the hydrophobic motif by Mst2 and autophosphorylation of the activation loop. We plan to compare phosphorylation of these two residues between the Lats1 truncated variants and wt Lats1 using Western blot analysis. Once we have validated the function of the minimal units of the N and C-

termini of Lats1, we will clone the minimal, functional unit of Lats1. We will purify the minimal, functional unit of Lats1 to both study the kinase activity of Lats1 *in vitro* and resolve the structure of the Lats1 variant bound to Mob1.

Second, we examined the molecular role of Mob1 in Lats1 kinase activation. Recent studies have shown that not only does Mob1 binding to Lats1 enhance both substrate phosphorylation and autophosphorylation, but Mob1 also stimulates phosphorylation of Lats1 by Mst2 (Ni et al., 2015). We validated this result by transiently transfecting HEK293 cells with Mst2, Lats1, and Mob1 and detecting T1079 phosphorylation by Western blot analysis. Mob1 co-expression stimulated T1079 phosphorylation within the hydrophobic motif. Ni et al. hypothesized that Mob1 mediates the formation of a ternary complex to stimulate hydrophobic motif phosphorylation by Mst2 as the binding sites for Mst2 and Lats1 within the Mob1 core domain do not intersect (Ni et al., 2015).

Although the ternary complex has been isolated *in vitro* using gel filtration chromatography, we still have many questions concerning the role of Mob1 in the activation of Lats1 kinase (Ni et al., 2015). We seek to answer whether the phosphorylation state of Mob1 affects ternary complex formation as phosphorylation results in Mob1 conformational change. Thus far, we have purified the Lats1 MBD and designed experiments to conduct pull-down experiments *in vitro*. We plan to purify phosphorylated and unphosphorylated Mob1 as well as Mst2 for use in the pull-down experiment. Also, we will inhibit the binding interactions within the ternary complex by expressing mutants of Lats1, Mst2, and Mob1 in HEK293 cells to observe how disruption of ternary complex formation affects phosphorylation of Lats1 by Mst2. With these

results, we will be able to validate whether ternary complex formation mediates the stimulation of Lats1 phosphorylation by Mst2 observed with Mob1 co-expression. Due to time constraints, we were unable to complete and report these experiments here.

References

Malakhov, M. P. *et al.* SUMO fusions and SUMO-specific protease for efficient expression and purification of proteins. *J Struct Func Genom* **5,** 75–86.

Plouffe, S. W., Hong, A. W. & Guan, K.-L. Disease implications of the Hippo/YAP pathway. *Trends in Molecular Medicine* **21,** 212–222 (2015).

Pearce, L. R., Komander, D. & Alessi, D. R. The nuts and bolts of AGC protein kinases. *Nat Rev Mol Cell Biol* **11,** 9–22 (2010).

Hergovich, A. Regulation and functions of mammalian LATS/NDR kinases: looking beyond canonical Hippo signalling. *Cell Biosci* **3,** 32 (2013).

Berggård, T., Linse, S. & James, P. Methods for the detection and analysis of protein–protein interactions. *Proteomics* **7,** 2833–2842 (2007).

Saucedo, L. J. & Edgar, B. A. Filling out the Hippo pathway. *Nat Rev Mol Cell Biol* **8,** 613–621 (2007).

Kessler, S. W. Rapid Isolation of Antigens from Cells with A Staphylococcal Protein A-Antibody Adsorbent: Parameters of the Interaction of Antibody-Antigen Complexes with Protein A. *J Immunology* **115,** 1617–1624 (1975).

Yabuta, N. *et al.* Structure, Expression, and Chromosome Mapping of LATS2, a Mammalian Homologue of the Drosophila Tumor Suppressor Gene lats/warts. *Genomics* **63,** 263–270 (2000).

Sjobring, U., Bjorck, L. & Kastern, W. Streptococcal Protein G. *J. Biol. Chem.* **266,** 399–405 (1991).

Stegert, M. R., Hergovich, A., Tamaskovic, R., Bichsel, S. J. & Hemmings, B. A. Regulation of NDR Protein Kinase by Hydrophobic Motif Phosphorylation Mediated by the Mammalian Ste20-Like Kinase MST3. *Molecular and Cellular Biology* **25,** 11019–11029 (2005).

Eliasson, M., Andersson, R., Olsson, A., Wigzell, H. & Uhlen, M. Differential IgG-binding characteristics of staphylococcal protein A, streptococcal protein G, and a chimeric protein AG. *J Immunology* **142,** 575–581 (1989).

Jia, J. The Drosophila Ste20 family kinase dMST functions as a tumor suppressor by restricting cell proliferation and promoting apoptosis. *Genes & Development* **17,** 2514 2519 (2003).

Tao, W. *et al.* Human homologue of the Drosophila melanogaster lats tumour suppressor modulates CDC2 activity. *Nat Genet* **21,** 177–181 (1999).

Björk, I., Petersson, B. Å. & Sjöquist, J. Some Physicochemical Properties of Protein A from Staphylococcus aureus. *European Journal of Biochemistry* **29,** 579–584 (1972).

Drozdetskiy, A., Cole, C., Procter, J. & Barton, G. J. JPred4: a protein secondary structure prediction server. *Nucleic Acids Res* **43,** W389–W394 (2015).

Zhao, B. *et al.* TEAD mediates YAP-dependent gene induction and growth control. *Genes & Development* **22,** 1962–1971 (2008).

Vrabioiu, A. M. & Struhl, G. Fat/Dachsous Signaling Promotes Drosophila Wing Growth by Regulating the Conformational State of the NDR Kinase Warts. *Developmental Cell* **35,** 737–749 (2015).

Chan, E. H. Y. *et al.* The Ste20-like kinase Mst2 activates the human large tumor suppressor kinase Lats1. *Oncogene* **24,** 2076–2086 (2005).

Structural Genomics Consortium *et al.* Protein production and purification. *Nat Methods* **5,** 135–146 (2008).

St John, M. A. R. *et al.* Mice deficient of Lats1 develop soft-tissue sarcomas, ovarian tumours and pituitary dysfunction. *Nat Genet* **21,** 182–186 (1999).

Isono, E. & Schwechheimer, C. in *Plant Developmental Biology* (eds. Hennig, L. & Köhler, C.) **655,** 377–387 (Humana Press, 2010).

Udan, R. S., Kango-Singh, M., Nolo, R., Tao, C. & Halder, G. Hippo promotes proliferation arrest and apoptosis in the Salvador/Warts pathway. *Nat Cell Biol* **5,** 914–920 (2003).

Camargo, F. D. *et al.* YAP1 Increases Organ Size and Expands Undifferentiated Progenitor Cells. *Current Biology* **17,** 2054–2060 (2007).

Stegert, M. R., Tamaskovic, R., Bichsel, S. J., Hergovich, A. & Hemmings, B. A. Regulation of NDR2 Protein Kinase by Multi-site Phosphorylation and the S100B Calcium-binding Protein. *J. Biol. Chem.* **279,** 23806–23812 (2004).

Wu, S., Huang, J., Dong, J. & Pan, D. hippo Encodes a Ste-20 Family Protein Kinase that Restricts Cell Proliferation and Promotes Apoptosis in Conjunction with salvador and warts. *Cell* **114,** 445–456 (2003).

Tamaskovic, R., Bichsel, S. J. & Hemmings, B. A. NDR family of AGC kinases—essential regulators of the cell cycle and morphogenesis. *FEBS Lett.* **546,** 73–80 (2003).

Kim, S.-Y., Tachioka, Y., Mori, T. & Hakoshima, T. Structural basis for autoinhibition and its relief of MOB1 in the Hippo pathway. *Sci Rep* **6,** 267 (2016).

Galan, J. A. & Avruch, J. MST1/MST2 Protein Kinases: Regulation and Physiologic Roles. *Biochemistry* **55,** 5507–5519 (2016).

Sievers, F. *et al.* Fast, scalable generation of high-quality protein multiple sequence alignments using Clustal Omega. *Molecular Systems Biology* **7,** 539–539 (2011).

Millward, T. A., Hess, D. & Hemmings, B. A. Ndr Protein Kinase Is Regulated by Phosphorylation on Two Conserved Sequence Motifs. *J. Biol. Chem.* **274,** 33847–33850 (1999).

Drozdetskiy, A., Cole, C., Procter, J. & Barton, G. J. JPred4: a protein secondary structure prediction server. *Nucleic Acids Res* **43,** W389–W394 (2015).

Ni, L. *et al.* Structural Basis for Autoactivation of Human Mst2 Kinase and Its Regulation by RASSF5. *Structure* **21,** 1757–1768 (2013).

Stegert, M. R., Hergovich, A., Tamaskovic, R., Bichsel, S. J. & Hemmings, B. A. Regulation of NDR Protein Kinase by Hydrophobic Motif Phosphorylation Mediated by the Mammalian Ste20-Like Kinase MST3. *Molecular and Cellular Biology* **25,** 11019–11029 (2005).

Xiong, S. *et al.* Regulation of Protein Interactions by Mps One Binder (MOB1) Phosphorylation. *Mol Cell Proteomics* **16,** 1111–1125 (2017).

Dong, J. *et al.* Elucidation of a Universal Size-Control Mechanism in Drosophila and Mammals. *Cell* **130,** 1120–1133 (2007).

Kohler, R. S., Schmitz, D., Cornils, H., Hemmings, B. A. & Hergovich, A. Differential NDR/LATS Interactions with the Human MOB Family Reveal a Negative Role for Human MOB2 in the Regulation of Human NDR Kinases. *Molecular and Cellular Biology* **30,** 4507–4520 (2010).

Gógl, G. *et al.* The Structure of an NDR/LATS Kinase–Mob Complex Reveals a Novel Kinase–Coactivator System and Substrate Docking Mechanism. *PLoS Biol* **13,** e1002146 (2015).

ZHANG, H.-C., YANG, J., YANG, G.-W., WANG, X.-J. & FAN, H.-T. Production of recombinant protein G through high-density fermentation of engineered bacteria as well as purification. *Molecular Medicine Reports* **12,** 3132–3138 (2015).

Ni, L., Zheng, Y., Hara, M., Pan, D. & Luo, X. Structural basis for Mob1-dependent activation of the core Mst-Lats kinase cascade in Hippo signaling. *Genes & Development* **29,** 1416–1431 (2015).

Takahashi, Y. in *Plant Developmental Biology* (eds. Hennig, L. & Köhler, C.) **1278,** 381–389 (Springer New York, 2015).

Bichsel, S. J., Tamaskovic, R., Stegert, M. R. & Hemmings, B. A. Mechanism of Activation of NDR (Nuclear Dbf2-related) Protein Kinase by the hMOB1 Protein. *J. Biol. Chem.* **279,** 35228–35235 (2004).

Yu, T., Bachman, J. & Lai, Z.-C. Evidence for a Tumor Suppressor Role for the Large Tumor Suppressor Genes LATS1and LATS2in Human Cancer. *Genetics* **195,** 1193–1196 (2013).

Eliasson, M., Andersson, R., Nygren, P.-A. & Uhlen, M. Structural and functional analysis of the human IgG-Fab receptor activity of streptococcal protein G. *Molecular Immunology* **28,** 1055–1061 (1991).

Nishio, M. *et al.* Cancer susceptibility and embryonic lethality in Mob1a/1b double-mutant mice. *J. Clin. Invest.* **122,** 4505–4518 (2012).

Björck, L., Kastern, W., Lindahl, G. & Widebäck, K. Streptococcal protein G, expressed by streptococci or by Escherichia coli, has separate binding sites for human albumin and IgG. *Molecular Immunology* **24,** 1113–1122 (1987).

Wei, X., Shimizu, T. & Lai, Z.-C. Mob as tumor suppressor is activated by Hippo kinase for growth inhibition in Drosophila. *EMBO J* **26,** 1772–1781 (2007).

Dong, J. Differences in Yes-associated protein and mRNA levels in regenerating liver and hepatocellular carcinoma. *Molecular Medicine Reports* **5,** 410–414 (2011).

Hao, Y., Chun, A., Cheung, K., Rashidi, B. & Yang, X. Tumor Suppressor LATS1 Is a Negative Regulator of Oncogene YAP. *J. Biol. Chem.* **283,** 5496–5509 (2008).

Couzens, A. L. *et al.* MOB1 Mediated Phospho-recognition in the Core Mammalian Hippo Pathway. *Mol Cell Proteomics* **16,** 1098–1110 (2017).

Bothos, J., Tuttle, R. L., Ottey, M., Luca, F. C. & Halazonetis, T. D. Human LATS1 is a mitotic exit network kinase. *Cancer Res.* **65,** 6568–6575 (2005).

Praskova, M., Xia, F. & Avruch, J. MOBKL1A/MOBKL1B Phosphorylation by MST1 and MST2 Inhibits Cell Proliferation. *Current Biology* **18,** 311–321 (2008).

Markham, K., Bai, Y. & Schmitt-Ulms, G. Co-immunoprecipitations revisited: an update on experimental concepts and their implementation for sensitive interactome investigations of endogenous proteins. *Anal Bioanal Chem* **389,** 461–473 (2007).

Dong, J. Differences in Yes-associated protein and mRNA levels in regenerating liver and hepatocellular carcinoma. *Molecular Medicine Reports* **5,** 410–414 (2011).

Harvey, K. F., Pfleger, C. M. & Hariharan, I. K. The Drosophila Mst Ortholog, hippo, Restricts Growth and Cell Proliferation and Promotes Apoptosis. *Cell* **114,** 457–467 (2003).

Devroe, E., Erdjument-Bromage, H., Tempst, P. & Silver, P. A. Human Mob Proteins Regulate the NDR1 and NDR2 Serine-Threonine Kinases. *J. Biol. Chem.* **279,** 24444–24451 (2004).

Xu, T., Wang, W., Zhang, S., Stewart, R. A. & Yu, W. Identifying tumor suppressors in genetic mosaics: the Drosophila lats gene encodes a putative protein kinase. *Development* **121,** 1053–1063 (1995).

Hergovich, A., Schmitz, D. & Hemmings, B. A. The human tumour suppressor LATS1 is activated by human MOB1 at the membrane. *Biochemical and Biophysical Research Communications* **345,** 50–58 (2006).

Kulaberoglu, Y. *et al.* Stable MOB1 interaction with Hippo/MST is not essential for development and tissue growth control. *Nat Commun* **8,** 63 (2017).

Lai, Z.-C. *et al.* Control of Cell Proliferation and Apoptosis by Mob as Tumor Suppressor, Mats. *Cell* **120,** 675–685 (2005).

Huang, J., Wu, S., Barrera, J., Matthews, K. & Pan, D. The Hippo Signaling Pathway Coordinately Regulates Cell Proliferation and Apoptosis by Inactivating Yorkie, the Drosophila Homolog of YAP. *Cell* **122,** 421–434 (2005).

Bjorck, L. & Kronvall, G. Purification and some properties of streptococcal protein G, a novel IgG-binding reagent. *J Immunology* **133,** 969–974 (1984).

Hoa, L. *et al.* The characterisation of LATS2 kinase regulation in Hippo-YAP signalling. *Cellular Signalling* **28,** 488–497 (2016).

Cook, D., Hoa, L. Y., Gomez, V., Gomez, M. & Hergovich, A. Constitutively active NDR1-PIF kinase functions independent of MST1 and hMOB1 signalling. *Cellular Signalling* **26,** 1657–1667 (2014).

Graille, M. *et al.* Crystal structure of a Staphylococcus aureus protein A domain complexed with the Fab fragment of a human IgM antibody: structural basis for recognition of B-cell receptors and superantigen activity. *Proceedings of the National Academy of Sciences* **97,** 5399–5404 (2000).

Ni, L., Zheng, Y., Hara, M., Pan, D. & Luo, X. Structural basis for Mob1-dependent activation of the core Mst–Lats kinase cascade in Hippo signaling. *Genes & Development* **29,** 1416–1431 (2015).

Johnson, M. Detergents: Triton X-100, Tween-20, and More. *MATER METHODS* **3,** (2013).

Justice, R. W., Zilian, O., Woods, D. F., Noll, M. & Bryant, P. J. The Drosophila tumor suppressor gene warts encodes a homolog of human myotonic dystrophy kinase and is required for the control of cell shape and proliferation. *Genes & Development* **9,** 534–546 (1995).

Kmiecik, S. & Kolinski, A. Folding Pathway of the B1 Domain of Protein G Explored by Multiscale Modeling. *Biophysical Journal* **94,** 726–736 (2008).

Halder, G. & Johnson, R. L. Hippo signaling: growth control and beyond. *Development* **138,** 9–22 (2010).

Bai, H. *et al.* Expression of Yes-associated protein modulates Survivin expression in primary liver malignancies. *Human Pathology* **43,** 1376–1385 (2012).

YOO JIN KIM

ykim121@jhu.edu; 847-560-0019

EDUCATION

Johns Hopkins University Bloomberg School of Public Health — May 2018
Department of Biochemistry and Molecular Biology — Baltimore, MD
Master of Science, GPA: 4.0
ScM Thesis: The molecular role of Mob1 in Lats1 kinase activation in Hippo signaling
Mentor: Jennifer M. Kavran, Ph.D.

Johns Hopkins University Krieger School of Arts and Sciences — May 2015
Bachelor of Science with Honors, GPA: 3.7 — Baltimore, MD
Neuroscience (Concentration: Cellular and Molecular) and Spanish

RESEARCH EXPERIENCE

Master of Science – Kavran Lab — Oct. 2016 – May 2018
Johns Hopkins University Bloomberg School of Public Health — Baltimore, MD

- Determined key structural and functional steps in Lats1/2 activity using cell-based assays.
- Developed a co-immunoprecipitation assay protocol and trained members of the Kavran Lab to use this assay.

Undergraduate Researcher – Lee Lab — Aug. 2014 – May 2015
Johns Hopkins University Krieger School of Arts and Sciences — Baltimore, MD

- Analyzed structural changes in thalamocortical projections that occur as a consequence of cross-modal sensory interactions in the adult brain using a mouse model.
- Developed an immunohistochemistry protocol.

Research Intern – Lesniak Lab — June 2013 – Aug. 2013
University of Chicago Pritzker School of Medicine — Chicago, IL

- Assisted the discovery of future immunotherapeutic targets for the treatment of malignant glioma using a mouse model.

CLINICAL EXPERIENCE

Volunteer – Bon Secours Hospital — Feb. 2017 – May 2018
Baltimore, MD

- Visited patients and their families with the hospitality cart.
- Organized donations to extend the $200 monthly hospitality cart budget.

Volunteer – St. Alexius Medical Center — Feb. 2016 – Aug. 2016
Hoffman Estates, IL

- Bridged the communication between physicians and patients' families at the day surgery center.
- Supported patients throughout their stay at the orthopedic in-patient floor: coordinated therapy dog visits, answered call lights, and organized linens and patient forms.

Physician Shadowing – St. Alexius Medical Center — Aug. 2016
- Clinical shadowing in the Department of Radiation Oncology — Hoffman Estates, IL

Physician Shadowing – Good Samaritan Hospital — Jan. 2015 – May 2015
- Clinical shadowing in the Department of Cardiology — Baltimore, MD

Volunteer and Medical Interpreter – Chang-Dong Hospital — May 2013 – Aug. 2013
- Interpreted symptoms, concerns, and questions for English-speaking patients.
- Escorted and supported patients throughout their stay at the hospital. — South Korea

Clinical Observation – Samsung Hospital — May 2012 – Aug. 2012
- Clinical shadowing in the Department of Neurosurgery — South Korea

COMMUNITY SERVICE AND LEADERSHIP EXPERIENCE

Master of Science Program (ScM) Student Representative – Aug. 2017 – May 2018
Johns Hopkins University Bloomberg School of Public Health, Department of Biochemistry and Molecular Biology — Baltimore, MD
- Shared the ScM students' interests, questions, and concerns with the faculty and staff.

Mentor – MERIT Health Leadership Academy — Feb. 2017 – May 2018
- Provided professional and academic support to underrepresented high school students interested in pursuing careers in science, health care, or medicine. — Baltimore, MD

AWARDS AND HONORS

Delta Omega Public Health Honor Society
Dean's List: Fall 2011, Spring 2012, Fall 2012, Spring 2013, Fall 2013, Fall 2014, Spring 2015

PUBLICATIONS

Cairns, L., Tran, T., Fowl, B., Patterson, A., **Kim, Y. J.**, Bothner, B., Kavran, J. Salvador has an extended SARAH domain that mediates binding to Hippo kinase. *J. Biol. Chem.* jbc.RA117.000923 (2018). doi:10.1074/jbc.RA117.000923